Highly dynamic marine redox states through the Cambrian explosion highlighted by authigenic $\delta^{238}U$ records

Guang-Yi Wei[1,2*], Noah J. Planavsky[2], Lidya G. Tarhan[2], Tianchen He[3], Dan Wang[4], Graham A. Shields[5], Wei Wei[6], Hong-Fei Ling[1*]

[1]State Key Laboratory for Mineral Deposits Research, School of Earth Sciences and Engineering, Nanjing University, 163 Xianlin Avenue, Nanjing 210023, China
[2]Department of Geology and Geophysics, Yale University, New Haven, CT 06520, USA
[3]School of Earth and Environment, University of Leeds, Leeds, U.K.
[4]School of Geographic Science, Nantong University, Nantong 226019, China
[5]Department of Earth Sciences, University College London, Gower Street, London WC1E 6BT, U.K.
[6]CAS Key Laboratory of Crust-Mantle Materials and Environments, School of Earth and Space Sciences, University of Science and Technology of China, Anhui 230026, China

*Guang-Yi Wei (guangyiwei@nju.edu.cn); Hong-Fei Ling (hfling@nju.edu.cn)

Abstract

The history of oceanic oxygenation from the late Neoproterozoic to the early Cambrian is currently debated, making it difficult to gauge whether, and to what extent environmental triggers played a role shaping the trajectory of metazoan diversification. Uranium isotope ($\delta^{238}U$) records from carbonates have recently been used to argue for significant swings in the global marine redox states from the late Neoproterozoic to the early Cambrian. However, geochemical signatures in carbonates—the U isotope archive most commonly employed to argue for redox shifts—are susceptible to diagenetic alteration and have variable offsets from seawater values. Therefore, there is an impetus to reconstruct seawater U isotopic evolution using another sedimentary archive, in order to crosscheck that these excursions can indeed be linked to global shifts in marine redox landscape. Here we report new U isotope data from two fine-grained siliciclastic upper Ediacaran to lower Cambrian (ca. 551 Ma–515 Ma) successions in South China. We find large $\delta^{238}U$ swings between -0.63‰ and +0.39‰ for calculated values of authigenic U in the siliciclastic rocks, consistent with correlative records from the carbonates. The replication of these patterns in both carbonate and siliciclastic units provides confirmatory~~compelling~~ evidence that the early Cambrian seawater was characterized by~~ did indeed experiences~~ highly ~~variable~~ variable U isotope compositions~~marine redox conditions~~. These new $\delta^{238}U$ data also provide higher-resolution records of global oceanic redox during ~~the~~ Cambrian Age 3, coeval with a critical interval of the Cambrian explosion. These $\delta^{238}U$ data bolster the case that the Ediacaran-Cambrian transition~~ did indeed~~ experienced massive swings in marine redox state, providing a dynamic environmental backdrop for and potentially even a key driver of the emergence and radiation of metazoans.

Keywords

uranium isotopes; siliciclastic strata; early Cambrian; marine redox dynamics; animal innovations

1. Introduction

There has been longstanding debate over~~regarding~~ whether the Ediacaran–Cambrian emergence and diversification of metazoans coincided with progressive oxidation of the ocean-atmosphere system and, if so, to what extent this environmental transition may have directly influenced the trajectory or pace of metazoan evolution (Och and Shields-Zhou, 2012; Lyons et al., 2014; Sperling et al., 2013, 2015). In contrast to the standard view of a largely unidirectional redox transition, several recent studies have suggested that, during the interval spanning the Ediacaran to the early Cambrian, pulses~~d episodes~~ of widespread marine anoxia were common and recurrent (Wei et al., 2018; Wood et al., 2018; Zhang et al., 2018, 2019; Tostevin et al., 2019; Dahl et al., 2019). Building upon~~from~~ this emerging record of environmental variability, it has been suggested that temporally and spatially dynamic environmental conditions, rather than stymying the emergence of complex life, actually spurred the development and dissemination of biotic novelties, and thus the rapid diversification, ~~and~~ turnover and ecosystem restructuring characteristic of this interval (Wei et al., 2018; Wood and Erwin, 2018; Wood et al., 2019). Uranium (U) isotopes have played a key role in reconstructing ancient marine redox landscapes, based on the framework that seawater U isotopic compositions are controlled by the balance between~~of~~ different marine U sinks with distinct isotopic fractionations relative to seawater (Andersen et al., 2017). For instance, extensive euxinia (anoxic and sulfidic conditions) in open-ocean settings will drive seawater towards very light dissolved U isotopic compositions~~;~~, whereas more limited euxinic and extensive oxygenated waters result in isotopically heavier seawater~~ with heavy U isotope values~~ (*Andersen et al., 2017*). Marine carbonates record seawater U isotope values—providing a seemingly ideal and simple means of tracking global oceanic redox evolution. To date marine carbonates have been the chief geologic archive for reconstructing global seawater U isotope compositions from the Ediacaran to the

Cambrian Age 2 (ca. 635–520 Ma) (Wei et al., 2018; Zhang et al., 2018, 2019; Tostevin et al., 2019; Dahl et al., 2019). However, carbonate-hosted U isotopes can be extensively modified during ~~the~~ diagenesis. Early marine diagenesis typically results in more positive carbonate U isotope values, but late-stage alteration of carbonates can result in more negative U isotope values (e.g., Hood et al., 2016, 2018; Chen et al., 2018; Tissot et al., 2018), which can hamper the use of carbonate as a seawater archive. Therefore, there is an obvious motivation to explore other U isotope archives to track global marine redox evolution.

Modern reducing sediments generally document higher $\delta^{238}U$ values, relative to seawater (Weyer et al., 2008; Andersen et al., 2014; Holmden et al., 2015; Abshire et al., 2020; Brüske et al., 2020) because ^{238}U is preferentially reduced and accumulates in reducing sediments via microbially mediated reduction of U (VI) (e.g. Basu et al., 2014; Stirling et al., 2015; Stylo et al., 2015). Observed U isotopic differences between reducing sediments and seawater are sensitive to variations in local depositional environment, including local productivity and sedimentation rates, basin connectivity and bottom-water redox state (Bura-Nakić et al., 2018; Andersen et al., 2018; Brüske et al., 2020; Lau et al., 2020), which adds complexity to precise reconstruction of seawater $\delta^{238}U$ values. However, given that exposure to reducing conditions will result in higher $\delta^{238}U$ values in the sediments relative to seawater, reducing sediments can provide a robust maximum estimate for seawater values. Further, integration of $\delta^{238}U$ analysis of reducing sediments with detailed characterization of the hosting facies can be used to track secular changes in seawater

$\delta^{238}U$ values. In this light, shale- and mudstone-hosted U isotope records can be used to independently test whether the widespread anoxia reconstructed for the Ediacaran and Cambrian, on the basis of carbonate archives, accurately reflects ancient marine conditions.

In this study, we report new high-resolution $\delta^{238}U$ data from two marine siliciclastic successions (Daotuo drill core and Yanjia section) (Fig. 1) in the Yangtze block, South China, which span the terminal Ediacaran to Cambrian Stage 3 (ca. 551–515 Ma). We focus on U-enriched silicified shale~~shaly chert~~, shale and mudstone, given that the presence of authigenic U enrichments in these lithologies can provide an archive of seawater $\delta^{238}U$ values, independent of~~from~~ that of shallow carbonates. We measured $\delta^{238}U$ values from these lithologies, and coupled these to trace element and iron speciation analyses, in order to provide new insights into global seawater $\delta^{238}U$ evolution and compare these to carbonate $\delta^{238}U$ records.

2. Geological background

The Daotuo drill core, collected from Songtao County of northeastern Guizhou Province, South China, is interpreted to record a weakly restricted mid-depth slope environment during the early Cambrian (Wei et al., 2017). The studied Daotuo drill core samples were collected from the upper Liuchapo Formation to the Jiumenchong Formation, which comprise~~consist of~~ black chert, black shale, mudstone and calcareous mudstone (Fig. 1). The upper Liuchapo Formation spans the Ediacaran-Cambrian boundary (ca. 542 Ma), based on ~~a~~ U-Pb zircon geochronology~~dating~~ (Chen et al., 2015a). The lower Jiumenchong Formation contains a polymetallic sulfide-rich layer whose age is 521 ± 5 Ma based on Re-Os daing (Xu et al., 2011) or younger than 522.7 ± 4.9 Ma based on U-Pb zircon dating (Wang et al., 2012) of~~for the~~ correlated strata in other sections from South China. The Yanjia section is exposed in Chun'an County of Zhejiang Province, South China and interpreted to have been deposited in a deep basin, relatively well connected to the open ocean (Wang et al., 2018). The Yanjia section comprises the Piyuancun Formation and the overlying Hetang Formation, both of which are composed of organic-rich chert, siliceous shale and black shale. The Piyuancun and Hetang formations in the Yanjia section can be correlated to the Liuchapo and Jiumenchong ormations in the Daotuo drill core section, respectively (cf. Wang et al., 2018).

Stratigraphic correlations on the Yangtze block are shown in Fig. 1, including two sections from the inner shelfal and intrashelf basinal settings (Wei et al., 2018). The studied strata of the Daotuo drill core and Yanjia section are highly condensed in the Cambrian Fortunian and Stage 2 (ca. 541–521 Ma), ~~which are age equivalent to~~compared with more expanded ~~-~~carbonate successions in the Xiaotan and Yanjiahe sections (cf. Wei et al., 2018; Dahl et al., 2019). Most samples in this study (middle and upper Jiumenchong and Hetang formations) were deposited during Cambrian Age 3 (ca. 520–515 Ma), an interval during which deposition of chert, black shale and siliceous-calcareous mudstones was widespread across the Yangtze block.

3. Materials and methods

The studied samples with relatively low Ca concentrations (< 3%) were carefully selected~~petrographically screened~~ in order to avoid~~for~~ the effects of any carbonate components and obvious late-stage veins, and then analyzed for U isotopic composition as well as trace element concentration and total organic carbon. HF, HNO_3 and HCl acids were used to fully digest the samples. Trace element concentrations of the studied samples were measured on a Thermo Finnigan Element XR ICP-MS at Yale University and Nanjing University with errors lower than 5%. Uranium isotopes were measured on a Thermo Finnigan Neptune Plus MC-ICP-MS at Yale University following column chromatography using UTEVA resin, using the method described in Wei et al. (2018). Long-term reproducibility was better than 0.07‰ (2SD), based on replications of the NOD-A-1 geostandard (-0.61‰ ± 0.05, n = 5) and CRM 112a standard (0.03‰ ± 0.07, n = 42).

From among the studied samples for U isotope analyses, representative ones were selected for iron speciation analyses in order to further constrain the local redox conditions. ~~-~~Iron speciation analyses were completed~~finished~~ at Nanjing University and Nanjing Institute of Geology and Palaeontology, Chinese Academy of Sciences, following the sequential extraction procedure of Poulton and Canfield (2005) in order to analyze highly reactive Fe in carbonate, oxides and magnetite, and following the Cr-reduction method of Canfield et al. (1986) for extraction of pyrite-associated Fe. Iron concentrations of extracted highly reactive Fe were measured on an atomic absorption spectroscope (AAS) and ICP-OES with errors lower than 5%. The yield of pyrite- Fe was better than 90% based on ~~the~~ repeated analyses of the Chinese GBW07267 pyrite standard. ~~The d~~Details of all~~ the~~ analytical methods are shown in the Supplementary Materials.

4. Results and discussion

4.1 Uranium isotopes in uppermost Ediacaran through lower Cambrian fine-grained siliciclastic strata: local depositional or global marine redox control?

Results of U isotope, Fe speciation, total organic carbon and trace element concentration analyses are shown in Table S1 and Fig. 2. High bulk U/Th ratios (distinctly higher than those of terrestrial detrital materials, $U/Th_{detrital} = 0.282 \pm 0.102$, 2SD) (Cole et al., 2017) and~~ no~~ a lack of any clear covariation~~correlations~~ between bulk U concentrations ($[U]_{bulk}$), bulk $\delta^{238}U$ values ($\delta^{238}U_{bulk}$) and Al or Th concentrations (Fig. 3~~A, B, C, D~~) suggest only negligible ~~trivial~~ detrital ~~U~~ contribution to our reported U isotope signatures~~ produced from the analyzed samples~~. We therefore interpret measured $\delta^{238}U$ signatures to record the behavior of predominantly authigenic (seawater-sourced) U deposited in the sediments under potentially anoxic conditions. In order to further disentangle marine authigenic signals from any potential detrital signals in the bulk sample U isotope data, we calculated U concentrations and $\delta^{238}U$ values of marine authigenic uranium ($[U]_{auth}$ and $\delta^{238}U_{auth}$), by using the equations published in Andersen et al. (2017) with a simple Monte Carlo simulation to evaluate the uncertainties on calculated $\delta^{238}U_{auth}$ values (see Supplementary materials for detail). The Daotuo drill core and Yanjia section exhibit consistent trends and a wide range~~ but consistently varying trend~~ of $\delta^{238}U_{auth}$ values from -0.63‰ to +0.39‰ and from -0.42‰ to +0.32‰, respectively (Fig. 2). Although

$[U]_{auth}$ and $\delta^{238}U_{auth}$ of the studied samples vary greatly in the Daotuo and Yanjia sections, no covariation between $[U]_{auth}$ and ~~$\delta^{238}U_{auth}$ values show no correlation with~~ Fe contents ~~(Fig. 3E, F)~~but clear covariation between $[U]_{auth}$ and TOC (total organic carbon) contents (Fig. 4) likely ~~, which likely~~ suggests that U precipitation was dominated by bacterially mediated U reduction, rather than abiotic Fe (II)-mediated U reduction (e.g., Stylo et al., 2015), which highlights the importance of organic substrates on U precipitation in the anoxic sediments (e.g., Tribovillard et al., 2006).

Samples from the lowest Jiumenchong and Hetang formations (upper Cambrian Stage 2), show strongly positive $\delta^{238}U_{auth}$ values (up to +0.39‰) (Fig. 2), equivalent to or slightly higher than the heaviest reported U isotope compositions of modern euxinic sediments (e.g., as high as that of Black Sea unit II) (Andersen et al., 2014). Although the units with high $\delta^{238}U_{auth}$ values in the lowest Jiumenchong and Hetang formations display relatively~~significantly~~ high $[U]_{auth}$ and ~~total organic carbon (~~TOC~~)~~ contents (Figs. 2 and 4), given the lack of significant covariation between $\delta^{238}U_{auth}$ and TOC (Fig. 4D), such high $\delta^{238}U_{auth}$ values (up to +0.39‰) are unlikely to have been driven primarily by high organic carbon burial fluxes because increased organic carbon delivery within the sediments generally results in rapid U reduction and more quantitative precipitation of U in the sediments, reducing the U isotopic fractionation between sediments and seawater (Andersen et al., 2018; Brüske et al., 2020; Lau et al., 2020). Instead, we suggest that this stratigraphic interval records greater water column or water-sediment interface reduction of U (rather than reduction within the sediment pile) under highly productive conditions, which is consistent with the U isotopic behavior expected in very highly ~~-~~productive regions (cf. Rolison et al., 2017; Abshire et al., 2020; Cheng et al., 2020). Uranium reduction in an unrestricted water column or at the water–sediment interface may result in a higher effective U isotopic fractionation between the sediment and coeval~~concurrent~~ seawater (Rolison et al., 2017; Andersen et al., 2017; Brüske et al., 2020; Abshire et al., 2020). Nonetheless, even if the U isotope offset between sediment and seawater $\delta^{238}U$ was~~is~~ large, comparable to the largest offsets (~ 0.8‰) observed in modern anoxic depositional systems (Rolison et al., 2017; Brüske et al., 2020), high $\delta^{238}U_{auth}$ values (up to +0.39‰) recorded here likely reflect near-modern seawater $\delta^{238}U$ values. In this view, high seawater $\delta^{238}U$ values in this interval indicate~~suggest~~ a relatively limited extent of anoxic seawater during late Cambrian Age 2, which is consistent with previously published Mo isotope records (Chen et al., 2015b).

In contrast, the Liuchapo and upper Piyuancun formations and the middle to upper Jiumenchong and Hetang formations are marked by low $\delta^{238}U_{auth}$ values (< -0.6‰) that are notably lower than that of modern seawater (Fig. 2). In fact, these are the most negative shale U isotopic values (as low as -0.63‰) that have ever been reported (cf. Wang et al., 2018). These values likely reflect nearly complete U reduction (which can occur in an isolated basin or in porewaters beneath suboxic bottom water). With near quantitative capture of a U reservoir, $\delta^{238}U_{auth}$ values of sediments can approach that of seawater (Noordmann et al., 2015; Andersen et al., 2016, 2018; Bura-Nakić et al., 2018). However, even if there is no appreciable U isotopic difference between sediments and seawater, the remarkably negative $\delta^{238}U_{auth}$

values in the Liuchapo and upper Piyuancun formations and middle to upper Jiumenchong and Hetang formations imply remarkably~~markedly~~ low seawater $\delta^{238}U$ values (as low as -0.63‰) across the Ediacaran-Cambrian boundary and during Cambrian Age 3, suggesting widespread marine anoxia during these intervals.

To further determine local depositional conditions and thus constrain U isotopic differences between open seawater and the local sediments, we conducted iron speciation analyses (Fe_{HR}/Fe_T and Fe_{Py}/Fe_{HR}) and Mo, U enrichment factors (Mo_{EF} and U_{EF}) (see Supplementary materials for calculations). Using the standard iron speciation framework (Poulton and Canfield, 2011), essentially all the samples included in this study were deposited under anoxic—but not persistently and strongly sulfidic—bottom water (Fig. 5~~4~~A). We do not observe any systematic relationships between $\delta^{238}U_{auth}$ and Fe_{HR}/Fe_T, Fe_{Py}/Fe_{HR} (Fig. 6~~5~~), which suggests that redox conditions of local bottom water may have not been the dominant factor controlling $\delta^{238}U_{auth}$ values of the studied samples. Covariation of Mo_{EF} and U_{EF} is used to further evaluate the depositional environment of the samples in this study and to compare these with modern low-oxygen marine sedimentary systems (cf. Algeo and Tribovillard, 2009; Tribovillard et al., 2012). As shown in Fig. 5~~4~~B, most of the samples in this study fall within the iron speciation field characteristic of deposition under anoxic conditions and show a Mo_{EF}–U_{EF} trend analogous to that of modern open-ocean settings (cf. Algeo and Tribovillard, 2009; Tribovillard et al., 2012), which with the standard interpretation would suggest that the Yangtze continental margin was likely well-connected to the open ocean during the early Cambrian. A few samples with relatively low Mo_{EF} and U_{EF} values have significantly low $\delta^{238}U_{auth}$ values, potentially representing a locally suboxic ~~local~~ depositional environment with less U isotopic fractionation between the sediments and seawater. Collectively, these observations—Fe speciation and Mo_{EF}–U_{EF} covariation—imply that, during the early Cambrian, local bottom waters in these regions were well connected to the open ~~-~~ocean ~~waters~~ and experienced relatively prolonged intervals of strong anoxia. Taken together, we suggest that swings in $\delta^{238}U_{auth}$ values from the Daotuo drill core and Yanjia section were~~are~~ not solely controlled by local variability~~variation~~ in basin restriction, organic carbon delivery or bottom water redox conditions. Highly consistent $\delta^{238}U_{auth}$ variations in these two sections, in part, reflect frequent fluctuations in seawater $\delta^{238}U$ values. Most importantly~~Foremost~~, the anomalously positive $\delta^{238}U_{auth}$ values of~~in~~ upper Cambrian Stage 2 and negative $\delta^{238}U_{auth}$ values of~~in~~ Stage 3 strata provide evidence, independent of carbonate $\delta^{238}U$ records, for substantial~~intense and rapid~~ oscillations in~~of~~ oceanic redox states throughout the Cambrian explosion.

4.2 Reconstruction of seawater $\delta^{238}U$ from the late Ediacaran to early Cambrian via siliciclastic archives

Based on the above Fe speciation and Mo_{EF}–U_{EF} analyses, we reconstruct temporal changes in seawater U isotopic compositions ($\delta^{238}U_{SW}$, Fig. 7~~6~~C) from the reducing sedimentary records of this study by using +0.8‰, +0.6‰, +0.15‰, respectively, as the U isotopic offsets for 1) authigenic U reduction within the high-productive water column or water-sediment interface with efficient replenishment of dissolved U (Rolison et al., 2017; Brüske et al., 2020); 2) within sulfidic sediments of an unrestricted basin (Holmden et al., 2015; Andersen et al., 2018) and 3) within suboxic sediments~~–~~ (Weyer et al., 2008; Andersen et al., 2016). Although U isotopic behavior~~s~~ in~~ the~~ reducing sediments may be more complex, simplified estimation of U isotopic offsets under different local conditions can provide insights into secular changes in ancient $\delta^{238}U_{SW}$ values. Despite the relatively low-resolution nature of upper Ediacaran and Cambrian Fortunian $\delta^{238}U_{auth}$ data (e.g., three points from potentially suboxic samples for Fortunian excursion P1 in Fig. 7C) and the errors inherent to estimating an effective U isotopic fractionation, secular changes in $\delta^{238}U_{SW}$ reconstructed from siliciclastic rocks are strikingly consistent with correlative carbonate $\delta^{238}U$ profiles (Fig. 7~~6~~A). This supports the interpretation that changes in $\delta^{238}U_{auth}$ mainly reflect global oceanic redox changes. Further, compared to previous studies of carbonate-hosted U isotopic signatures (Fig. 7~~6~~A), the new $\delta^{238}U_{SW}$ curve documented in siliciclastic strata provides a higher-resolution record of global oceanic redox states through Cambrian Age 3, and suggests that this critical interval of the Cambrian explosion is marked by large swings in marine redox states.

4.3 Implications for co-evolution of marine environments and early metazoans

We provide estimates of late Ediacaran to early Cambrian (ca. 551 Ma–515 Ma) seawater $\delta^{238}U$ records from fine-grained siliciclastic rocks that closely match previous estimates from carbonates (Fig. 7~~6~~). This provides compelling evidence that the early Cambrian was indeed marked by frequent~~rapid~~ variations in seawater $\delta^{238}U$

(negative excursion N1–N3 and positive excursion P1–P3 in Fig. 7~~6~~). These swings demonstrate that there were largescale fluctuations in the marine redox landscape (with the U mass balance being tied foremost to the areal extent of anoxic conditions). The frequently fluctuating redox states of the early Cambrian ocean are likely linked to effects of dynamic nutrient supply, shallow marine productivity and ocean ventilation in the ocean with relatively lower baseline oxygenation level than the modern ocean (cf. Wang et al., 2018; He et al., 2019; Dahl et al., 2019; Wei et al., 2020). Further studies are needed to better constrain the triggers for the dramatic changes in marine redox states during this period. The synchronicity of this dynamic redox variation with animal evolutionary~~l~~ clades, increased physiological and ecological complexity and expansion into a wider range of benthic habitats and water depths may, moreover, not be coincidental. In fact, this concurrence provides further empirical evidence in favor of recent proposals that habitat fragmentation and ecological restructuring mediated by redox instability may have facilitated higher rates of generation of evolutionary novelties and thus enhanced biological innovation and turnover—thus serving as a spur, rather than an impediment, to diversification among animal lineages over this interval (Reinhard et al., 2016; Wood and Erwin, 2018). In this light, rather than being an anomalous episode in Earth's history, the Ediacaran–Cambrian protracted emergence and subsequent rapid radiations of complex animal life (and Ediacaran–Ordovician emergence of modern-style ecological strategies and ecosystem structure) against a backdrop of pronounced environmental instability (Droser et al., 2017; Tarhan et a., 2018; Servais and Harper, 2018; Wood et al., 2019), broadly resembles patterns of emergence and turnover characteristic of Sepkoskian Phanerozoic Evolutionary Faunas (e.g., Tarhan et al., 2018).

5. Conclusions

New high-resolution uranium isotope data from two upper Ediacaran through Cambrian Stage 3 siliciclastic sections in South China are reported in this study. Both of the studied sections show mutually consistent,~~ly~~ large swings in authigenic $\delta^{238}U$ values. Given that local depositional conditions did~~may have~~ not dominate~~d~~ authigenic $\delta^{238}U$ values of the studied samples, we interpret much of this variability to be driven by secular changes in seawater $\delta^{238}U$ values. Notably high authigenic $\delta^{238}U$ values in upper Cambrian Stage 2 and lowest Stage 3 suggest that host sediments were deposited in and ocean with limited anoxic seafloor area~~anoxia~~, whereas anomalously negative authigenic $\delta^{238}U$ values in the terminal Ediacaran and Cambrian Stage 3 are indicative of extensive deep-marine anoxia. Paired $\delta^{238}U$ records from marine carbonates (Wei et al., 2018; Zhang et al., 2018; Tostevin et al., 2019; Dahl et al., 2019) and siliciclastic strata strengthens the case that anomalously high $\delta^{238}U$ variability (e.g., Wei et al., 2018; Dahl et al., 2019) is~~ indeed~~ tied to episodic~~the frequent~~ swings in global marine redox states from the late Ediacaran through the early Cambrian (ca. 551 Ma–510 Ma), rather than~~instead of~~ diagenetic overprinting. This bolsters the hypothesis that the diversification of early animals during the Cambrian explosion occurred against a backdrop of (and may even have been mediated by) highly spatiotemporally variable marine redox conditions.

Acknowledgements

This work was funded by the National Natural Science Foundation of China (NSFC) program 41872002, the Strategic Priority Research Program (B) of the Chinese Academy of Sciences (CAS) (XDB26000000) and NSFC program 41661134048 (China-UK BETR programme). Guang-Yi Wei thanks the fund by the program A for Outstanding PhD. Candidate of Nanjing University (No.201802A020). Dan Wang thanks the fund by NSFC program 41603023. Wei Wei thanks the fund by NSFC program 41902025. We also thank Editor Frederic Moynier for handling this paper; Dr. Huan Cui and an anonymous reviewer for constructive reviews that greatly improved this paper.

References

Abshire, M.L., Romaniello, S.J., Kuzminov, A.M., Cofrancesco, J., Severmann, S., Riedinger, N., 2020. Uranium isotopes as a proxy for primary depositional redox conditions in organic-rich marine systems. Earth and Planetary Science Letters 529, 115878.

Algeo, T.J., Tribovillard, N., 2009. Environmental analysis of paleoceanographic systems based on molybdenum–uranium covariation. Chemical Geology 268, 211-225.

Andersen, M.B., Romaniello, S., Vance, D., Little, S.H., Herdman, R., Lyons, T.W., 2014. A modern framework for the interpretation of 238U/235U in studies of ancient ocean redox. Earth and Planetary Science Letters 400, 184-194.

Andersen, M.B., Stirling, C. H., Weyer, S., 2017. Uranium Isotope Fractionation.

Reviews in Mineralogy and Geochemistry 82, 799-850.

Andersen, M.B., Vance, D., Morford, J.L., Bura-Nakić, E., Breitenbach, S.F.M., Och, L., 2016. Closing in on the marine 238U/235U budget. Chemical Geology 420, 11-22.

Andersen, M.B., Matthews, A., Vance, D., Bar-Matthews, M., Archer, C., de Souza, G.F., 2018. A 10-fold decline in the deep Eastern Mediterranean thermohaline overturning circulation during the last interglacial period. Earth and Planetary Science Letters 503, 58-67.

Basu, A., Sanford, R. A., Johnson, T. M., Lundstrom, C. C., Loffler, F. E., 2014. Uranium isotopic fractionation factors during U(VI) reduction by bacterial isolates. Geochemica et Cosmochimica Acta 136, 100-113.

Brüske, A., Weyer, S., Zhao, M.Y., Planavsky, N.J., Wegwerth, A., Neubert, N., Dellwig, O., Lau, K.V., Lyons, T.W., 2020. Correlated molybdenum and uranium isotope signatures in modern anoxic sediments: Implications for their use as paleo-redox proxy. Geochimica et Cosmochimica Acta 270, 449-474.

Bura-Nakić, E., Andersen, M.B., Archer, C., de Souza, G.F., Marguš, M., Vance, D., 2018. Coupled Mo-U abundances and isotopes in a small marine euxinic basin: Constraints on processes in euxinic basins. Geochimica et Cosmochimica Acta 222, 212-229.

Canfield, D.E., Raiswell, R., Westrich, J.T., Reaves, C.M., Berner, R.A., 1986. The use of chromium reduction in the analysis of reduced inorganic sulfur in sediments and shales. Chemical Geology 54, 149-155.

Chen, D., Zhou, X., Fu, Y., Wang, J., Yan, D., 2015a. New U-Pb zircon ages of the Ediacaran-Cambrian boundary strata in South China. Terra Nova 27, 62-68.

Chen, X., Ling, H.F., Vance, D., Shields-Zhou, G.A., Zhu, M., Poulton, S.W., Och, L.M., Jiang, S.Y., Li, D., Cremonese, L., Archer, C., 2015b. Rise to modern levels of ocean oxygenation coincided with the Cambrian radiation of animals. Nat Commun 6, 7142.

Chen, X., Romaniello, S.J., Herrmann, A.D., Hardisty, D., Gill, B.C., Anbar, A.D., 2018. Diagenetic effects on uranium isotope fractionation in carbonate sediments from the Bahamas. Geochimica et Cosmochimica Acta 237, 294-311.

Cheng, M., Li, C., Jin, C., Wang, H., Algeo, T.J., Lyons, T.W., Zhang, F., Anbar, A., 2020. Evidence for high organic carbon export to the early Cambrian seafloor. Geochimica et Cosmochimica Acta. In press.

Cole, D.B., Zhang, S., Planavsky, N.J., 2017. A new estimate of detrital redox-sensitive metal concentrations and variability in fluxes to marine sediments. Geochimica Et Cosmochimica Acta 215, 337-353.

Dahl, T.W., Connelly, J.N., Li, D., Kouchinsky, A., Gill, B.C., Porter, S., Maloof, A.C., Bizzarro, M., 2019. Atmosphere-ocean oxygen and productivity dynamics during early animal radiations. Proc. Natl. Acad. Sci. USA 116, 19352-19361.

Droser, M.L., Tarhan, L.G., Gehling, J.G., 2017. The Rise of Animals in a Changing Environment: Global Ecological Innovation in the Late Ediacaran. Annual Review of Earth and Planetary Sciences 45, 593-617.

He, T., Zhu, M., Mills, B.J.W., Wynn, P.M., Zhuravlev, A.Y., Tostevin, R., Pogge von

Strandmann, P.A.E., Yang, A., Poulton, S.W., Shields, G.A., 2019. Possible links between extreme oxygen perturbations and the Cambrian radiation of animals. Nature Geoscience 12, 468-474.

Holmden, C., Amini, M., Francois, R., 2015. Uranium isotope fractionation in Saanich Inlet: A modern analog study of a paleoredox tracer. Geochimica et Cosmochimica Acta 153, 202-215.

Hood, A.v.S., Planavsky, N.J., Wallace, M.W., Wang, X., Bellefroid, E.J., Gueguen, B., Cole, D.B., 2016. Integrated geochemical-petrographic insights from component-selective δ238U of Cryogenian marine carbonates. Geology 44, 935-938.

Hood, A.v.S., Planavsky, N.J., Wallace, M.W., Wang, X., 2018. The effects of diagenesis on geochemical paleoredox proxies in sedimentary carbonates. Geochimica et Cosmochimica Acta 232, 265-287.

Lau, K.V., Lyons, T.W., Maher, K., 2020. Uranium reduction and isotopic fractionation in reducing sediments: Insights from reactive transport modeling. Geochimica et Cosmochimica Acta. In press.

Lyons, T.W., Reinhard, C.T., Planavsky, N.J., 2014. The rise of oxygen in Earth's early ocean and atmosphere. Nature 506, 307-315.

Noordmann, J., Weyer, S., Montoya-Pino, C., Dellwig, O., Neubert, N., Eckert, S., Paetzel, M., Böttcher, M.E., 2015. Uranium and molybdenum isotope systematics in modern euxinic basins: Case studies from the central Baltic Sea and the Kyllaren fjord (Norway). Chemical Geology 396, 182-195.

Och, L.M., Shields-Zhou, G.A., 2012. The Neoproterozoic oxygenation event: Environmental perturbations and biogeochemical cycling. Earth-Science Reviews 110, 26-57.

Poulton, S., Canfield, D., 2005. Development of a sequential extraction procedure for iron: implications for iron partitioning in continentally derived particulates. Chemical Geology 214, 209-221.

Poulton, S.W., Canfield, D.E., 2011. Ferruginous Conditions: A Dominant Feature of the Ocean through Earth's History. Elements 7, 107-112.

Reinhard, C.T., Planavsky, N.J., Olson, S.L., Lyons, T.W., Erwin, D.H., 2016. Earth's oxygen cycle and the evolution of animal life. Proc. Natl. Acad. Sci. USA 113, 8933-8938.

Rolison, J.M., Stirling, C.H., Middag, R., Rijkenberg, M.J.A., 2017. Uranium stable isotope fractionation in the Black Sea: Modern calibration of the 238U/235U paleo-redox proxy. Geochimica et Cosmochimica Acta 203, 69-88.

Servais, T., Harper, D.A.T., 2018. The Great Ordovician Biodiversification Event (GOBE): definition, concept and duration. Lethaia 51, 151-164.

Sperling, E.A., Frieder, C.A., Raman, A.V., Girguis, P.R., Levin, L.A., Knoll, A.H., 2013. Oxygen, ecology, and the Cambrian radiation of animals. Proc. Natl. Acad. Sci. USA 110, 13446-13451.

Sperling, E.A., Knoll, A.H., Girguis, P.R., 2015. The Ecological Physiology of Earth's Second Oxygen Revolution. Annual Review of Ecology, Evolution, and Systematics 46, 215-235.

Stirling, C.H., Andersen, M.B., Warthmann, R., Halliday, A.N., 2015. Isotope fractionation of ^{238}U and ^{235}U during biologically-mediated uranium reduction. Geochimica et Cosmochimica Acta 163, 200-218.

Stylo, M., Neubert, N., Wang, Y., Monga, N., Romaniello, S.J., Weyer, S., Bernier-Latmani, R., 2015. Uranium isotopes fingerprint biotic reduction. Proc. Natl. Acad. Sci. USA 112, 5619-5624.

Tarhan, L.G., Droser, M.L., Cole, D.B., Gehling, J.G., 2018. Ecological Expansion and Extinction in the Late Ediacaran: Weighing the Evidence for Environmental and Biotic Drivers. Integr. Comp. Biol. 58, 688-702.

Tissot, F.L.H., Chen, C., Go, B.M., Naziemiec, M., Healy, G., Bekker, A., Swart, P.K., Dauphas, N., 2018. Controls of eustasy and diagenesis on the 238U/235U of carbonates and evolution of the seawater (234U/238U) during the last 1.4 Myr. Geochimica et Cosmochimica Acta 242, 233-265.

Tostevin, R., Clarkson, M.O., Gangl, S., Shields, G.A., Wood, R.A., Bowyer, F., Penny, A.M., Stirling, C.H., 2019. Uranium isotope evidence for an expansion of anoxia in terminal Ediacaran oceans. Earth and Planetary Science Letters 506, 104-112.

Tribovillard, N., Algeo, T.J., Baudin, F., Riboulleau, A., 2012. Analysis of marine environmental conditions based onmolybdenum–uranium covariation—Applications to Mesozoic paleoceanography. Chemical Geology 324-325, 46-58.

Tribovillard, N., Algeo, T.J., Lyons, T., Riboulleau, A., 2006. Trace metals as paleoredox and paleoproductivity proxies: An update. Chemical Geology 232, 12-32.

Wang, D., Ling, H.-F., Struck, U., Zhu, X.-K., Zhu, M., He, T., Yang, B., Gamper, A., Shields, G. A., 2018a. Coupling of ocean redox and animal evolution during the Ediacaran-Cambrian transition. Nature Communications 9, 2575.

Wang, X.L., Planavsky, N.J., Hofmann, A., Saupe, E.E., De Corte, B.P., Philippot, P., LaLonde, S.V., Jemison, N.E., Zou, H.J., Ossa, F.O., Rybacki, K., Alfimova, N., Larson, M.J., Tsikos, H., Fralick, P.W., Johnson, T.M., Knudsen, A.C., Reinhard, C.T., Konhauser, K.O., 2018b. A Mesoarchean shift in uranium isotope systematics. Geochimica Et Cosmochimica Acta 238, 438-452.

Wang, X., Shi, X., Jiang, G., Zhang, W., 2012. New U–Pb age from the basal Niutitang Formation in South China: Implications for diachronous development and condensation of stratigraphic units across the Yangtze platform at the Ediacaran–Cambrian transition. Journal of Asian Earth Sciences 48, 1-8.

Wei, G.-Y., Ling, H.-F., Li, D., Wei, W., Wang, D., Chen, X., Zhu, X.-K., Zhang, F.-F., Yan, B., 2017. Marine redox evolution in the early Cambrian Yangtze shelf margin area: evidence from trace elements, nitrogen and sulphur isotopes. Geological Magazine 154, 1344-1359.

Wei, G.-Y., Planavsky, N.J., Tarhan, L.G., Chen, X., Wei, W., Li, D., Ling, H.-F., 2018. Marine redox fluctuation as a potential trigger for the Cambrian explosion. Geology 46, 587-590.

Wei, G.-Y., Wei, W., Wang, D., Li, T., Yang, X., Shields, G.A., Zhang, F., Li, G., Chen, T., Yang, T., Ling, H.-F., 2020. Enhanced chemical weathering triggered an expansion of euxinic seawater in the aftermath of the Sturtian glaciation. Earth and Planetary Science Letters 539, 116244.

Weyer, S., Anbar, A.D., Gerdes, A., Gordon, G.W., Algeo, T.J., Boyle, E.A., 2008. Natural fractionation of $^{238}U/^{235}U$. Geochimica et Cosmochimica Acta 72, 345-359.

Wood, R., Bowyer, F., Penny, A., Poulton, S.W., 2018. Did anoxia terminate Ediacaran benthic communities? Evidence from early diagenesis. Precambrian Research 313, 134-147.

Wood, R., Erwin, D.H., 2018. Innovation not recovery: dynamic redox promotes metazoan radiations. Biol. Rev. Camb. Philos. Soc. 93, 863-873.

Wood, R., Liu, A.G., Bowyer, F., Wilby, P.R., Dunn, F.S., Kenchington, C.G., Cuthill, J.F.H., Mitchell, E.G., Penny, A., 2019. Integrated records of environmental change and evolution challenge the Cambrian Explosion. Nat. Ecol. Evol. 3, 528-538.

Xu, L., Lehmann, B., Mao, J.,Qu, W., Du, A., 2011. Re-Os Age of Polymetallic Ni-Mo-PGE-Au Mineralization in Early Cambrian Black Shales of South China--A Reassessment. Economic Geology 106, 511-522.

Zhang, F., Xiao, S., Kendall, B., Romaniello, S.J., Cui, H., Meyer, M., Gilleaudeau, G.J., Kaufman, A.J., Anbar, A.D., 2018. Extensive marine anoxia during the terminal Ediacaran Period. Science Advances 4, eaan8983.

Zhang, F., Xiao, S., Romaniello, S.J., Hardisty, D., Li, C., Melezhik, V., Pokrovsky, B., Cheng, M., Shi, W., Lenton, T.M., Anbar, A.D., 2019. Global marine redox changes drove the rise and fall of the Ediacara biota. Geobiology 17, 594-610.

Figure captions

Figure 1. Stratigraphic columns of the Daotuo drill core and Yanjia sections, and their correlations to inner shelf Xiaotan section and Gaojiaxi–Yanjiahe section in South China (cf. Wei et al., 2018). The shaded areas represent the correlative stratigraphic units of these sections for the Ediacaran (blue), Cambrian Fortunian and Stage 2 (green) and Stage 3 (yellow). The red line represents a Ni-Mo polymetallic layer with an age of 521± 5 Ma (Re-Os dating from Xu et al., 2011) or < 522.7 ± 4.9 Ma (U-Pb zircon dating from Wang et al., 2012).

Figure 2. Uranium isotope ($\delta^{238}U_{auth}$) values, iron speciation, U_{auth} concentrations and total organic carbon (TOC) contents of the upper Ediacaran to lower Cambrian Daotuo drill core and Yanjia section. Uranium isotope values are presented as $\delta^{238}U_{auth}$ for authigenic uranium in bulk samples. $\delta^{238}U_{auth}$ calculation are shown in Supplementary materials. The error bar represents an overall uncertainty (2SD) of calculated $\delta^{238}U_{auth}$ for each sample, using a Monte Carlo approach. The shaded vertical bars are estimated average $\delta^{238}U$ ranges of suboxic and euxinic sediments (Andersen et al., 2017).

Figure 3. Cross-plots of (A) bulk U concentration vs. Al concentration, (B) bulk $\delta^{238}U$ vs. Al concentration, (C) bulk U concentration vs. Th concentration, (D) bulk $\delta^{238}U$ vs. Th concentration~~, (E) authigenic U concentration vs. Fe concentration, (F) authigenic $\delta^{238}U$ vs. Fe concentration~~ for samples from the Daotuo drill core and Yanjia section. R^2 represents the

coefficient of determination of the covariation.

Figure 4. Cross plots of (A) authigenic U concentration vs. Fe concentration, (B) authigenic $\delta^{238}U$ vs. Fe concentration, (C) authigenic U concentration vs. TOC concentration, (D) authigenic $\delta^{238}U$ vs. TOC concentration for samples from the Daotuo drill core and Yanjia section. R^2 represents the coefficient of determination of the covariation.

Figure 5~~4~~. (A) Fe_{HR}/Fe_T vs. Fe_{Py}/Fe_{HR} for the samples from the Daotuo drill core and Yanjia section analyzed in this study. The divisions between oxic and anoxic conditions (Fe_{HR}/Fe_T = 0.22–0.38) and between ferruginous and euxinic conditions (Fe_{Py}/Fe_{HR} = 0.7–0.8) are derived from Poulton and Canfield (2011). (B) Cross-plots of Mo_{EF} vs. U_{EF} for the samples from the Daotuo drill core and Yanjia section in this study as a proxy for local marine sedimentary environment. The shaded zones for different sedimentary environment of the modern ocean are modified after Algeo and Tribovillard (2009) and Tribovillard et al. (2012). Particulate shuttle zone: the transport of Mo within the water column by Fe-Mn-oxyhydroxide particulates (e.g., as in the Cariaco Basin); Open marine zone: benthic redox variations in modern open-ocean systems; Strongly restricted basin: sedimentary basin weakly connected to the open-ocean (e.g, as in the Black Sea).

Figure 6~~5~~. Cross-plots of (A) authigenic $\delta^{238}U$ vs. Fe_{HR}/Fe_T, (B) authigenic $\delta^{238}U$ vs. Fe_{Py}/Fe_{HR} for the samples in the Daotuo drill core and Yanjia section.

Figure 7~~6~~. (A)–(B) Secular changes in U isotopic compositions of carbonates (data from Wei et al., 2018; Zhang et al., 2018; Tostevin et al., 2019; Dahl et al., 2019) and siliciclastic rocks from the late Ediacaran to early Cambrian. (C) Calculated $\delta^{238}U_{SW}$ values derived from $\delta^{238}U_{auth}$ records in this study. The solid curves are LOWESS smoothing fits for U isotope data. Based on TOC, Mo_{EF}–U_{EF} and Fe speciation analyses, U isotopic differences between reducing sediment and seawater are estimated to be +0.8‰ for organic-rich anoxic or sulfidic samples with TOC > 5 wt% and Mo_{EF} and U_{EF} > 20 (purple circles); +0.6‰ for anoxic samples with TOC < 5wt%, Mo_{EF} and U_{EF} >10 (orange circles); and +0.15‰ for potentially suboxic samples with Mo_{EF} and U_{EF} < 10 (gray circles). The shaded vertical bars are estimated average $\delta^{238}U$ ranges of modern non-skeletal carbonates, suboxic sediments and euxinic sediments (Andersen et al., 2017). N1–N3 and P1–P3 represent negative and positive U isotopic excursions from the late Ediacaran though the early Cambrian.

Highlights

- High-resolution U isotope data from early Cambrian siliciclastic sections
- Global marine redox changes dominate U isotopes of the studied samples
- Frequent marine redox fluctuations likely trigger the early animal innovation

Highly dynamic marine redox states through the Cambrian explosion highlighted by authigenic $\delta^{238}U$ records

Guang-Yi Wei[1,2*], Noah J. Planavsky[2], Lidya G. Tarhan[2], Tianchen He[3], Dan Wang[4], Graham A. Shields[5], Wei Wei[6], Hong-Fei Ling[1*]

[1]State Key Laboratory for Mineral Deposits Research, School of Earth Sciences and Engineering, Nanjing University, 163 Xianlin Avenue, Nanjing 210023, China
[2]Department of Geology and Geophysics, Yale University, New Haven, CT 06520, USA
[3]School of Earth and Environment, University of Leeds, Leeds, U.K.
[4]School of Geographic Science, Nantong University, Nantong 226019, China
[5]Department of Earth Sciences, University College London, Gower Street, London WC1E 6BT, U.K.
[6]CAS Key Laboratory of Crust-Mantle Materials and Environments, School of Earth and Space Sciences, University of Science and Technology of China, Anhui 230026, China

*Guang-Yi Wei (guangyiwei@nju.edu.cn); Hong-Fei Ling (hfling@nju.edu.cn)

Abstract

The history of oceanic oxygenation from the late Neoproterozoic to the early Cambrian is currently debated, making it difficult to gauge whether, and to what extent environmental triggers played a role shaping the trajectory of metazoan diversification. Uranium isotope ($\delta^{238}U$) records from carbonates have recently been used to argue for significant swings in the global marine redox states from the late Neoproterozoic to the early Cambrian. However, geochemical signatures in carbonates—the U isotope archive most commonly employed to argue for redox shifts—are susceptible to diagenetic alteration and have variable offsets from seawater values. Therefore, there is an impetus to reconstruct seawater U isotopic evolution using another sedimentary archive, in order to crosscheck that these excursions can indeed be linked to global shifts in marine redox landscape. Here we report new U isotope data from two fine-grained siliciclastic upper Ediacaran to lower Cambrian (ca. 551 Ma–515 Ma) successions in South China. We find large $\delta^{238}U$ swings between -0.63‰ and +0.39‰ for calculated values of authigenic U in the siliciclastic rocks, consistent with correlative records from the carbonates. The replication of these patterns in both carbonate and siliciclastic units provides confirmatory evidence that the early Cambrian seawater was characterized by highly variable U isotope compositions. These new $\delta^{238}U$ data also provide higher-resolution records of global oceanic redox during Cambrian Age 3, coeval with a critical interval of the Cambrian explosion. These $\delta^{238}U$ data bolster the case that the Ediacaran-Cambrian transition experienced massive swings in marine redox state, providing a dynamic environmental backdrop for and potentially even a key driver of the emergence and radiation of metazoans.

Keywords

uranium isotopes; siliciclastic strata; early Cambrian; marine redox dynamics; animal innovations

1. Introduction

There has been longstanding debate over whether the Ediacaran–Cambrian emergence and diversification of metazoans coincided with progressive oxidation of the ocean-atmosphere system and, if so, to what extent this environmental transition may have directly influenced the trajectory or pace of metazoan evolution (Och and Shields-Zhou, 2012; Lyons et al., 2014; Sperling et al., 2013, 2015). In contrast to the standard view of a largely unidirectional redox transition, several recent studies have suggested that, during the interval spanning the Ediacaran to the early Cambrian, pulses of widespread marine anoxia were common and recurrent (Wei et al., 2018; Wood et al., 2018; Zhang et al., 2018, 2019; Tostevin et al., 2019; Dahl et al., 2019). Building upon this emerging record of environmental variability, it has been suggested that temporally and spatially dynamic environmental conditions, rather than stymying the emergence of complex life, actually spurred the development and dissemination of biotic novelties, and thus the rapid diversification, turnover and ecosystem restructuring characteristic of this interval (Wei et al., 2018; Wood and Erwin, 2018; Wood et al., 2019). Uranium (U) isotopes have played a key role in reconstructing ancient marine redox landscapes, based on the framework that seawater U isotopic compositions are controlled by the balance between different marine U sinks with distinct isotopic fractionations relative to seawater (Andersen et al., 2017). For instance, extensive euxinia (anoxic and sulfidic conditions) in open-ocean settings will drive seawater towards very light dissolved U isotopic compositions, whereas more limited euxinic and extensive oxygenated waters result in isotopically heavier seawater (*Andersen et al., 2017*). Marine carbonates record seawater U isotope values—providing a seemingly ideal and simple means of tracking global oceanic redox evolution. To date marine carbonates have been the chief geologic archive for reconstructing global seawater U isotope compositions from the Ediacaran to the Cambrian Age 2 (ca. 635–520 Ma) (Wei et al., 2018; Zhang et al., 2018, 2019; Tostevin et al., 2019; Dahl et al., 2019). However, carbonate-hosted U isotopes can be extensively modified during diagenesis. Early marine diagenesis typically results in more positive carbonate U isotope values, but late-stage alteration of carbonates can result in more negative U isotope values (e.g., Hood et al., 2016, 2018; Chen et al., 2018; Tissot et al., 2018), which can hamper the use of carbonate as a seawater archive. Therefore, there is an obvious motivation to explore other U isotope archives to track global marine redox evolution.

Modern reducing sediments generally document higher $\delta^{238}U$ values, relative to seawater (Weyer et al., 2008; Andersen et al., 2014; Holmden et al., 2015; Abshire et al., 2020; Brüske et al., 2020) because ^{238}U is preferentially reduced and accumulates in reducing sediments via microbially mediated reduction of U (VI) (e.g. Basu et al., 2014; Stirling et al., 2015; Stylo et al., 2015). Observed U isotopic differences between reducing sediments and seawater are sensitive to variations in local depositional environment, including local productivity and sedimentation rates, basin connectivity and bottom-water redox state (Bura-Nakić et al., 2018; Andersen et al., 2018; Brüske et al., 2020; Lau et al., 2020), which adds complexity to precise reconstruction of seawater $\delta^{238}U$ values. However, given that exposure to reducing conditions will result in higher $\delta^{238}U$ values in the sediments relative to seawater, reducing sediments can provide a robust maximum estimate for seawater values. Further, integration of $\delta^{238}U$ analysis of reducing sediments with detailed characterization of the hosting facies can be used to track secular changes in seawater $\delta^{238}U$ values. In this light, shale- and mudstone-hosted U isotope records can be used to independently test whether the widespread anoxia reconstructed for the Ediacaran and Cambrian, on the basis of carbonate archives, accurately reflects ancient marine conditions.

In this study, we report new high-resolution $\delta^{238}U$ data from two marine siliciclastic successions (Daotuo drill core and Yanjia section) (Fig. 1) in the Yangtze block, South China, which span the terminal Ediacaran to Cambrian Stage 3 (ca. 551–515 Ma). We focus on U-enriched silicified shale, shale and mudstone, given that the presence of authigenic U enrichments in these lithologies can provide an archive of seawater $\delta^{238}U$ values, independent of that of shallow carbonates. We measured $\delta^{238}U$ values from these lithologies, and coupled these to trace element and iron speciation analyses, in order to provide new insights into global seawater $\delta^{238}U$ evolution and compare these to carbonate $\delta^{238}U$ records.

2. Geological background

The Daotuo drill core, collected from Songtao County of northeastern Guizhou Province, South China, is interpreted to record a weakly restricted mid-depth slope environment during the early Cambrian (Wei et al., 2017). The studied Daotuo drill core samples were collected from the upper Liuchapo Formation to the Jiumenchong Formation, which comprise black chert, black shale, mudstone and calcareous mudstone (Fig. 1). The upper Liuchapo Formation spans the Ediacaran-Cambrian boundary (ca. 542 Ma), based on U-Pb zircon geochronology (Chen et al., 2015a). The lower Jiumenchong Formation contains a polymetallic sulfide-rich layer whose age is 521 ± 5 Ma based on Re-Os daing (Xu et al., 2011) or younger than 522.7 ± 4.9 Ma based on U-Pb zircon dating (Wang et al., 2012) of correlated strata in other sections from South China. The Yanjia section is exposed in Chun'an County of Zhejiang Province, South China and interpreted to have been deposited in a deep basin, relatively well connected to the open ocean (Wang et al., 2018). The Yanjia section comprises the Piyuancun Formation and the overlying Hetang Formation, both of which are composed of organic-rich chert, siliceous shale and black shale. The Piyuancun and Hetang formations in the Yanjia section can be correlated to the Liuchapo and Jiumenchong formations in the Daotuo drill core section, respectively (cf. Wang et al., 2018).

Stratigraphic correlations on the Yangtze block are shown in Fig. 1, including two sections from the inner shelfal and intrashelf basinal settings (Wei et al., 2018). The studied strata of the Daotuo drill core and Yanjia section are highly condensed in the Cambrian Fortunian and Stage 2 (ca. 541–521 Ma), compared with more expanded carbonate successions in the Xiaotan and Yanjiahe sections (cf. Wei et al., 2018; Dahl et al., 2019). Most samples in this study (middle and upper Jiumenchong and Hetang formations) were deposited during Cambrian Age 3 (ca. 520–515 Ma), an interval during which deposition of chert, black shale and siliceous-calcareous mudstones was widespread across the Yangtze block.

3. Materials and methods

The studied samples with relatively low Ca concentrations (< 3%) were carefully selected in order to avoid the effects of any carbonate components and obvious late-stage veins, and then analyzed for U isotopic composition as well as trace element concentration and total organic carbon. HF, HNO_3 and HCl acids were used to fully digest the samples. Trace element concentrations of the studied samples were measured on a Thermo Finnigan Element XR ICP-MS at Yale University and Nanjing University with errors lower than 5%. Uranium isotopes were measured on a Thermo Finnigan Neptune Plus MC-ICP-MS at Yale University following column chromatography using UTEVA resin, using the method described in Wei et al. (2018). Long-term reproducibility was better than 0.07‰ (2SD), based on replications of the NOD-A-1 geostandard (-0.61‰ ± 0.05, n = 5) and CRM 112a standard (0.03‰ ± 0.07, n = 42).

From among the studied samples for U isotope analyses, representative ones were selected for iron speciation analyses in order to further constrain the local redox conditions. Iron speciation analyses were completed at Nanjing University and Nanjing Institute of Geology and Palaeontology, Chinese Academy of Sciences, following the sequential extraction procedure of Poulton and Canfield (2005) in order to analyze highly reactive Fe in carbonate, oxides and magnetite, and following the Cr-reduction method of Canfield et al. (1986) for extraction of pyrite-associated Fe. Iron concentrations of extracted highly reactive Fe were measured on an atomic absorption spectroscope (AAS) and ICP-OES with errors lower than 5%. The yield of pyrite- Fe was better than 90% based on repeated analyses of the Chinese GBW07267 pyrite standard. Details of all analytical methods are shown in the Supplementary Materials.

4. Results and discussion

4.1 Uranium isotopes in uppermost Ediacaran through lower Cambrian

fine-grained siliciclastic strata: local depositional or global marine redox control?

Results of U isotope, Fe speciation, total organic carbon and trace element concentration analyses are shown in Table S1 and Fig. 2. High bulk U/Th ratios (distinctly higher than those of terrestrial detrital materials, $U/Th_{detrital} = 0.282 \pm 0.102$, 2SD) (Cole et al., 2017) and a lack of any clear covariation between bulk U concentrations ($[U]_{bulk}$), bulk $\delta^{238}U$ values ($\delta^{238}U_{bulk}$) and Al or Th concentrations (Fig. 3) suggest only negligible detrital contribution to our reported U isotope signatures. We therefore interpret measured $\delta^{238}U$ signatures to record the behavior of predominantly authigenic (seawater-sourced) U deposited in the sediments under potentially anoxic conditions. In order to further disentangle marine authigenic signals from any potential detrital signals in the bulk sample U isotope data, we calculated U concentrations and $\delta^{238}U$ values of marine authigenic uranium ($[U]_{auth}$ and $\delta^{238}U_{auth}$), by using the equations published in Andersen et al. (2017) with a simple Monte Carlo simulation to evaluate the uncertainties on calculated $\delta^{238}U_{auth}$ values (see Supplementary materials for detail). The Daotuo drill core and Yanjia section exhibit consistent trends and a wide range of $\delta^{238}U_{auth}$ values from -0.63‰ to +0.39‰ and from -0.42‰ to +0.32‰, respectively (Fig. 2). Although $[U]_{auth}$ and $\delta^{238}U_{auth}$ of the studied samples vary greatly in the Daotuo and Yanjia sections, no covariation between $[U]_{auth}$ and Fe contents but clear covariation between $[U]_{auth}$ and TOC (total organic carbon) contents (Fig. 4) likely suggests that U precipitation was dominated by bacterially mediated U reduction, rather than abiotic Fe (II)-mediated U reduction (e.g., Stylo et al., 2015), which highlights the importance of organic substrates on U precipitation in the anoxic sediments (e.g., Tribovillard et al., 2006).

Samples from the lowest Jiumenchong and Hetang formations (upper Cambrian Stage 2), show strongly positive $\delta^{238}U_{auth}$ values (up to +0.39‰) (Fig. 2), equivalent to or slightly higher than the heaviest reported U isotope compositions of modern euxinic sediments (e.g., as high as that of Black Sea unit II) (Andersen et al., 2014). Although the units with high $\delta^{238}U_{auth}$ values in the lowest Jiumenchong and Hetang formations display relatively high $[U]_{auth}$ and TOC contents (Figs. 2 and 4), given the lack of significant covariation between $\delta^{238}U_{auth}$ and TOC (Fig. 4D), such high $\delta^{238}U_{auth}$ values (up to +0.39‰) are unlikely to have been driven primarily by high organic carbon burial fluxes because increased organic carbon delivery within the sediments generally results in rapid U reduction and more quantitative precipitation of U in the sediments, reducing the U isotopic fractionation between sediments and seawater (Andersen et al., 2018; Brüske et al., 2020; Lau et al., 2020). Instead, we suggest that this stratigraphic interval records greater water column or water-sediment interface reduction of U (rather than reduction within the sediment pile) under highly productive conditions, which is consistent with the U isotopic behavior expected in very highly productive regions (cf. Rolison et al., 2017; Abshire et al., 2020; Cheng et al., 2020). Uranium reduction in an unrestricted water column or at the water–sediment interface may result in a higher effective U isotopic fractionation between the sediment and coeval seawater (Rolison et al., 2017; Andersen et al., 2017; Brüske et al., 2020; Abshire et al., 2020). Nonetheless, even if the U isotope offset between sediment and seawater $\delta^{238}U$ was large, comparable to the largest offsets (~ 0.8‰) observed in modern anoxic depositional systems (Rolison et al., 2017; Brüske et al., 2020), high $\delta^{238}U_{auth}$ values (up to +0.39‰) recorded here likely reflect near-modern seawater $\delta^{238}U$ values. In this view, high seawater $\delta^{238}U$ values in this interval indicate a relatively limited extent of anoxic seawater during late Cambrian Age 2, which is consistent with previously published Mo isotope records (Chen et al., 2015b).

In contrast, the Liuchapo and upper Piyuancun formations and the middle to upper Jiumenchong and Hetang formations are marked by low $\delta^{238}U_{auth}$ values (< -0.6‰) that are notably lower than that of modern seawater (Fig. 2). In fact, these are the most negative shale U isotopic values (as low as -0.63‰) that have ever been reported (cf. Wang et al., 2018). These values likely reflect nearly complete U reduction (which can occur in an isolated basin or in porewaters beneath suboxic bottom water). With near quantitative capture of a U reservoir, $\delta^{238}U_{auth}$ values of sediments can approach that of seawater (Noordmann et al., 2015; Andersen et al., 2016, 2018; Bura-Nakić et al., 2018). However, even if there is no appreciable U isotopic difference between sediments and seawater, the remarkably negative $\delta^{238}U_{auth}$ values in the Liuchapo and upper Piyuancun formations and middle to upper Jiumenchong and Hetang formations imply remarkably low seawater $\delta^{238}U$ values (as low as -0.63‰) across the Ediacaran-Cambrian boundary and during Cambrian Age 3, suggesting widespread marine anoxia during these intervals.

To further determine local depositional conditions and thus constrain U isotopic differences between open seawater and the local sediments, we conducted iron speciation analyses (Fe_{HR}/Fe_T and Fe_{Py}/Fe_{HR}) and Mo, U enrichment factors (Mo_{EF} and U_{EF}) (see Supplementary materials for calculations). Using the standard iron speciation framework (Poulton and Canfield, 2011), essentially all the samples included in this study were deposited under anoxic—but not persistently and strongly sulfidic—bottom water (Fig. 5A). We do not observe any systematic relationships between $\delta^{238}U_{auth}$ and Fe_{HR}/Fe_T, Fe_{Py}/Fe_{HR} (Fig. 6), which suggests that redox conditions of local bottom water may have not been the dominant factor controlling $\delta^{238}U_{auth}$ values of the studied samples. Covariation of Mo_{EF} and U_{EF} is used to further evaluate the depositional environment of the samples in this study and to compare these with modern low-oxygen marine sedimentary systems (cf. Algeo and Tribovillard, 2009; Tribovillard et al., 2012). As shown in Fig. 5B, most of the samples in this study fall within the iron speciation field characteristic of deposition under anoxic conditions and show a Mo_{EF}–U_{EF} trend analogous to that of modern open-ocean settings (cf. Algeo and Tribovillard, 2009; Tribovillard et al., 2012), which with the standard interpretation would suggest that the Yangtze continental margin was likely well-connected to the open ocean during the early Cambrian. A few samples with relatively low Mo_{EF} and U_{EF} values have significantly low $\delta^{238}U_{auth}$ values, potentially representing a locally suboxic depositional environment with less U isotopic fractionation between the sediments and seawater. Collectively, these observations—Fe speciation and Mo_{EF}–U_{EF} covariation—imply that, during the early Cambrian, local bottom waters in these regions were well connected to the open ocean and experienced relatively prolonged intervals of strong anoxia. Taken together, we suggest that swings in $\delta^{238}U_{auth}$ values from the Daotuo drill core and Yanjia section were not solely controlled by local variability in basin restriction, organic carbon delivery or bottom water redox conditions. Highly consistent $\delta^{238}U_{auth}$ variations in these two sections, in part, reflect frequent fluctuations in seawater $\delta^{238}U$ values. Most importantly, the anomalously positive $\delta^{238}U_{auth}$ values of upper Cambrian Stage 2 and negative $\delta^{238}U_{auth}$ values of Stage 3 strata provide evidence, independent of carbonate $\delta^{238}U$ records, for substantial oscillations in oceanic redox states throughout the Cambrian explosion.

4.2 Reconstruction of seawater δ^{238}U from the late Ediacaran to early Cambrian via siliciclastic archives

Based on the above Fe speciation and Mo_{EF}–U_{EF} analyses, we reconstruct temporal changes in seawater U isotopic compositions ($\delta^{238}U_{SW}$, Fig. 7C) from the reducing sedimentary records of this study by using +0.8‰, +0.6‰, +0.15‰, respectively, as the U isotopic offsets for 1) authigenic U reduction within the high-productive water column or water-sediment interface with efficient replenishment of dissolved U (Rolison et al., 2017; Brüske et al., 2020); 2) within sulfidic sediments of an unrestricted basin (Holmden et al., 2015; Andersen et al., 2018) and 3) within suboxic sediments (Weyer et al., 2008; Andersen et al., 2016). Although U isotopic behavior in reducing sediments may be more complex, simplified estimation of U isotopic offsets under different local conditions can provide insights into secular changes in ancient $\delta^{238}U_{SW}$ values. Despite the relatively low-resolution nature of upper Ediacaran and Cambrian Fortunian $\delta^{238}U_{auth}$ data (e.g., three points from potentially suboxic samples for Fortunian excursion P1 in Fig. 7C) and the errors inherent to estimating an effective U isotopic fractionation, secular changes in $\delta^{238}U_{SW}$ reconstructed from siliciclastic rocks are strikingly consistent with correlative carbonate $\delta^{238}U$ profiles (Fig. 7A). This supports the interpretation that changes in $\delta^{238}U_{auth}$ mainly reflect global oceanic redox changes. Further, compared to previous studies of carbonate-hosted U isotopic signatures (Fig. 7A), the new $\delta^{238}U_{SW}$ curve documented in siliciclastic strata provides a higher-resolution record of global oceanic redox states through Cambrian Age 3, and suggests that this critical interval of the Cambrian explosion is marked by large swings in marine redox states.

4.3 Implications for co-evolution of marine environments and early metazoans

We provide estimates of late Ediacaran to early Cambrian (ca. 551 Ma–515 Ma) seawater $\delta^{238}U$ records from fine-grained siliciclastic rocks that closely match previous estimates from carbonates (Fig. 7). This provides compelling evidence that the early Cambrian was indeed marked by frequent variations in seawater $\delta^{238}U$ (negative excursion N1–N3 and positive excursion P1–P3 in Fig. 7). These swings demonstrate that there were largescale fluctuations in the marine redox landscape (with the U mass balance being tied foremost to the areal extent of anoxic conditions). The frequently fluctuating redox states of the early Cambrian ocean are likely linked to effects of dynamic nutrient supply, shallow marine productivity and ocean ventilation in the ocean with relatively lower baseline oxygenation level than the modern ocean (cf. Wang et al., 2018; He et al., 2019; Dahl et al., 2019; Wei et al., 2020). Further studies are needed to better constrain the triggers for the dramatic changes in marine redox states during this period. The synchronicity of this dynamic redox variation with animal evolutionary clades, increased physiological and ecological complexity and expansion into a wider range of benthic habitats and water depths may, moreover, not be coincidental. In fact, this concurrence provides further empirical evidence in favor of recent proposals that habitat fragmentation and ecological restructuring mediated by redox instability may have facilitated higher rates of generation of evolutionary novelties and thus enhanced biological innovation and turnover—thus serving as a spur, rather than an impediment, to diversification among animal lineages over this interval (Reinhard et al., 2016; Wood and Erwin, 2018). In this light, rather than being an anomalous episode in Earth's history, the Ediacaran–Cambrian protracted emergence and subsequent rapid radiations of complex animal life (and Ediacaran–Ordovician emergence of modern-style ecological strategies and ecosystem structure) against a backdrop of pronounced environmental instability (Droser et al., 2017; Tarhan et a., 2018; Servais and Harper, 2018; Wood et al., 2019), broadly resembles patterns of emergence and turnover characteristic of Sepkoskian Phanerozoic Evolutionary Faunas (e.g., Tarhan et al., 2018).

5. Conclusions

New high-resolution uranium isotope data from two upper Ediacaran through Cambrian Stage 3 siliciclastic sections in South China are reported in this study. Both of the studied sections show mutually consistent, large swings in authigenic $\delta^{238}U$

values. Given that local depositional conditions did not dominate authigenic $\delta^{238}U$ values of the studied samples, we interpret much of this variability to be driven by secular changes in seawater $\delta^{238}U$ values. Notably high authigenic $\delta^{238}U$ values in upper Cambrian Stage 2 and lowest Stage 3 suggest that host sediments were deposited in and ocean with limited anoxic seafloor area, whereas anomalously negative authigenic $\delta^{238}U$ values in the terminal Ediacaran and Cambrian Stage 3 are indicative of extensive deep-marine anoxia. Paired $\delta^{238}U$ records from marine carbonates (Wei et al., 2018; Zhang et al., 2018; Tostevin et al., 2019; Dahl et al., 2019) and siliciclastic strata strengthens the case that anomalously high $\delta^{238}U$ variability (e.g., Wei et al., 2018; Dahl et al., 2019) is tied to episodic swings in global marine redox states from the late Ediacaran through the early Cambrian (ca. 551 Ma–510 Ma), rather than diagenetic overprinting. This bolsters the hypothesis that the diversification of early animals during the Cambrian explosion occurred against a backdrop of (and may even have been mediated by) highly spatiotemporally variable marine redox conditions.

Acknowledgements

This work was funded by the National Natural Science Foundation of China (NSFC) program 41872002, the Strategic Priority Research Program (B) of the Chinese Academy of Sciences (CAS) (XDB26000000) and NSFC program 41661134048 (China-UK BETR programme). Guang-Yi Wei thanks the fund by the program A for Outstanding PhD. Candidate of Nanjing University (No.201802A020). Dan Wang thanks the fund by NSFC program 41603023. Wei Wei thanks the fund by

NSFC program 41902025. We also thank Editor Frederic Moynier for handling this paper; Dr. Huan Cui and an anonymous reviewer for constructive reviews that greatly improved this paper.

References

Abshire, M.L., Romaniello, S.J., Kuzminov, A.M., Cofrancesco, J., Severmann, S., Riedinger, N., 2020. Uranium isotopes as a proxy for primary depositional redox conditions in organic-rich marine systems. Earth and Planetary Science Letters 529, 115878.

Algeo, T.J., Tribovillard, N., 2009. Environmental analysis of paleoceanographic systems based on molybdenum–uranium covariation. Chemical Geology 268, 211-225.

Andersen, M.B., Romaniello, S., Vance, D., Little, S.H., Herdman, R., Lyons, T.W., 2014. A modern framework for the interpretation of 238U/235U in studies of ancient ocean redox. Earth and Planetary Science Letters 400, 184-194.

Andersen, M.B., Stirling, C. H., Weyer, S., 2017. Uranium Isotope Fractionation. Reviews in Mineralogy and Geochemistry 82, 799-850.

Andersen, M.B., Vance, D., Morford, J.L., Bura-Nakić, E., Breitenbach, S.F.M., Och, L., 2016. Closing in on the marine 238U/235U budget. Chemical Geology 420, 11-22.

Andersen, M.B., Matthews, A., Vance, D., Bar-Matthews, M., Archer, C., de Souza, G.F., 2018. A 10-fold decline in the deep Eastern Mediterranean thermohaline overturning circulation during the last interglacial period. Earth and Planetary

Science Letters 503, 58-67.

Basu, A., Sanford, R. A., Johnson, T. M., Lundstrom, C. C., Loffler, F. E., 2014. Uranium isotopic fractionation factors during U(VI) reduction by bacterial isolates. Geochemica et Cosmochimica Acta 136, 100-113.

Brüske, A., Weyer, S., Zhao, M.Y., Planavsky, N.J., Wegwerth, A., Neubert, N., Dellwig, O., Lau, K.V., Lyons, T.W., 2020. Correlated molybdenum and uranium isotope signatures in modern anoxic sediments: Implications for their use as paleo-redox proxy. Geochimica et Cosmochimica Acta 270, 449-474.

Bura-Nakić, E., Andersen, M.B., Archer, C., de Souza, G.F., Marguš, M., Vance, D., 2018. Coupled Mo-U abundances and isotopes in a small marine euxinic basin: Constraints on processes in euxinic basins. Geochimica et Cosmochimica Acta 222, 212-229.

Canfield, D.E., Raiswell, R., Westrich, J.T., Reaves, C.M., Berner, R.A., 1986. The use of chromium reduction in the analysis of reduced inorganic sulfur in sediments and shales. Chemical Geology 54, 149-155.

Chen, D., Zhou, X., Fu, Y., Wang, J., Yan, D., 2015a. New U-Pb zircon ages of the Ediacaran-Cambrian boundary strata in South China. Terra Nova 27, 62-68.

Chen, X., Ling, H.F., Vance, D., Shields-Zhou, G.A., Zhu, M., Poulton, S.W., Och, L.M., Jiang, S.Y., Li, D., Cremonese, L., Archer, C., 2015b. Rise to modern levels of ocean oxygenation coincided with the Cambrian radiation of animals. Nat Commun 6, 7142.

Chen, X., Romaniello, S.J., Herrmann, A.D., Hardisty, D., Gill, B.C., Anbar, A.D.,

2018. Diagenetic effects on uranium isotope fractionation in carbonate sediments from the Bahamas. Geochimica et Cosmochimica Acta 237, 294-311.

Cheng, M., Li, C., Jin, C., Wang, H., Algeo, T.J., Lyons, T.W., Zhang, F., Anbar, A., 2020. Evidence for high organic carbon export to the early Cambrian seafloor. Geochimica et Cosmochimica Acta. In press.

Cole, D.B., Zhang, S., Planavsky, N.J., 2017. A new estimate of detrital redox-sensitive metal concentrations and variability in fluxes to marine sediments. Geochimica Et Cosmochimica Acta 215, 337-353.

Dahl, T.W., Connelly, J.N., Li, D., Kouchinsky, A., Gill, B.C., Porter, S., Maloof, A.C., Bizzarro, M., 2019. Atmosphere-ocean oxygen and productivity dynamics during early animal radiations. Proc. Natl. Acad. Sci. USA 116, 19352-19361.

Droser, M.L., Tarhan, L.G., Gehling, J.G., 2017. The Rise of Animals in a Changing Environment: Global Ecological Innovation in the Late Ediacaran. Annual Review of Earth and Planetary Sciences 45, 593-617.

He, T., Zhu, M., Mills, B.J.W., Wynn, P.M., Zhuravlev, A.Y., Tostevin, R., Pogge von Strandmann, P.A.E., Yang, A., Poulton, S.W., Shields, G.A., 2019. Possible links between extreme oxygen perturbations and the Cambrian radiation of animals. Nature Geoscience 12, 468-474.

Holmden, C., Amini, M., Francois, R., 2015. Uranium isotope fractionation in Saanich Inlet: A modern analog study of a paleoredox tracer. Geochimica et Cosmochimica Acta 153, 202-215.

Hood, A.v.S., Planavsky, N.J., Wallace, M.W., Wang, X., Bellefroid, E.J., Gueguen, B., Cole, D.B., 2016. Integrated geochemical-petrographic insights from component-selective δ238U of Cryogenian marine carbonates. Geology 44, 935-938.

Hood, A.v.S., Planavsky, N.J., Wallace, M.W., Wang, X., 2018. The effects of diagenesis on geochemical paleoredox proxies in sedimentary carbonates. Geochimica et Cosmochimica Acta 232, 265-287.

Lau, K.V., Lyons, T.W., Maher, K., 2020. Uranium reduction and isotopic fractionation in reducing sediments: Insights from reactive transport modeling. Geochimica et Cosmochimica Acta. In press.

Lyons, T.W., Reinhard, C.T., Planavsky, N.J., 2014. The rise of oxygen in Earth's early ocean and atmosphere. Nature 506, 307-315.

Noordmann, J., Weyer, S., Montoya-Pino, C., Dellwig, O., Neubert, N., Eckert, S., Paetzel, M., Böttcher, M.E., 2015. Uranium and molybdenum isotope systematics in modern euxinic basins: Case studies from the central Baltic Sea and the Kyllaren fjord (Norway). Chemical Geology 396, 182-195.

Och, L.M., Shields-Zhou, G.A., 2012. The Neoproterozoic oxygenation event: Environmental perturbations and biogeochemical cycling. Earth-Science Reviews 110, 26-57.

Poulton, S., Canfield, D., 2005. Development of a sequential extraction procedure for iron: implications for iron partitioning in continentally derived particulates. Chemical Geology 214, 209-221.

Poulton, S.W., Canfield, D.E., 2011. Ferruginous Conditions: A Dominant Feature of

the Ocean through Earth's History. Elements 7, 107-112.
Reinhard, C.T., Planavsky, N.J., Olson, S.L., Lyons, T.W., Erwin, D.H., 2016. Earth's oxygen cycle and the evolution of animal life. Proc. Natl. Acad. Sci. USA 113, 8933-8938.
Rolison, J.M., Stirling, C.H., Middag, R., Rijkenberg, M.J.A., 2017. Uranium stable isotope fractionation in the Black Sea: Modern calibration of the 238U/235U paleo-redox proxy. Geochimica et Cosmochimica Acta 203, 69-88.
Servais, T., Harper, D.A.T., 2018. The Great Ordovician Biodiversification Event (GOBE): definition, concept and duration. Lethaia 51, 151-164.
Sperling, E.A., Frieder, C.A., Raman, A.V., Girguis, P.R., Levin, L.A., Knoll, A.H., 2013. Oxygen, ecology, and the Cambrian radiation of animals. Proc. Natl. Acad. Sci. USA 110, 13446-13451.
Sperling, E.A., Knoll, A.H., Girguis, P.R., 2015. The Ecological Physiology of Earth's Second Oxygen Revolution. Annual Review of Ecology, Evolution, and Systematics 46, 215-235.
Stirling, C.H., Andersen, M.B., Warthmann, R., Halliday, A.N., 2015. Isotope fractionation of ^{238}U and ^{235}U during biologically-mediated uranium reduction. Geochimica et Cosmochimica Acta 163, 200-218.
Stylo, M., Neubert, N., Wang, Y., Monga, N., Romaniello, S.J., Weyer, S., Bernier-Latmani, R., 2015. Uranium isotopes fingerprint biotic reduction. Proc. Natl. Acad. Sci. USA 112, 5619-5624.
Tarhan, L.G., Droser, M.L., Cole, D.B., Gehling, J.G., 2018. Ecological Expansion

and Extinction in the Late Ediacaran: Weighing the Evidence for Environmental and Biotic Drivers. Integr. Comp. Biol. 58, 688-702.

Tissot, F.L.H., Chen, C., Go, B.M., Naziemiec, M., Healy, G., Bekker, A., Swart, P.K., Dauphas, N., 2018. Controls of eustasy and diagenesis on the 238U/235U of carbonates and evolution of the seawater (234U/238U) during the last 1.4 Myr. Geochimica et Cosmochimica Acta 242, 233-265.

Tostevin, R., Clarkson, M.O., Gangl, S., Shields, G.A., Wood, R.A., Bowyer, F., Penny, A.M., Stirling, C.H., 2019. Uranium isotope evidence for an expansion of anoxia in terminal Ediacaran oceans. Earth and Planetary Science Letters 506, 104-112.

Tribovillard, N., Algeo, T.J., Baudin, F., Riboulleau, A., 2012. Analysis of marine environmental conditions based onmolybdenum–uranium covariation—Applications to Mesozoic paleoceanography. Chemical Geology 324-325, 46-58.

Tribovillard, N., Algeo, T.J., Lyons, T., Riboulleau, A., 2006. Trace metals as paleoredox and paleoproductivity proxies: An update. Chemical Geology 232, 12-32.

Wang, D., Ling, H.-F., Struck, U., Zhu, X.-K., Zhu, M., He, T., Yang, B., Gamper, A., Shields, G. A., 2018a. Coupling of ocean redox and animal evolution during the Ediacaran-Cambrian transition. Nature Communications 9, 2575.

Wang, X.L., Planavsky, N.J., Hofmann, A., Saupe, E.E., De Corte, B.P., Philippot, P., LaLonde, S.V., Jemison, N.E., Zou, H.J., Ossa, F.O., Rybacki, K., Alfimova, N., Larson, M.J., Tsikos, H., Fralick, P.W., Johnson, T.M., Knudsen, A.C., Reinhard, C.T., Konhauser, K.O., 2018b. A Mesoarchean shift in uranium isotope systematics. Geochimica Et Cosmochimica Acta 238, 438-452.

Wang, X., Shi, X., Jiang, G., Zhang, W., 2012. New U–Pb age from the basal Niutitang Formation in South China: Implications for diachronous development and condensation of stratigraphic units across the Yangtze platform at the Ediacaran–Cambrian transition. Journal of Asian Earth Sciences 48, 1-8.

Wei, G.-Y., Ling, H.-F., Li, D., Wei, W., Wang, D., Chen, X., Zhu, X.-K., Zhang, F.-F., Yan, B., 2017. Marine redox evolution in the early Cambrian Yangtze shelf margin area: evidence from trace elements, nitrogen and sulphur isotopes. Geological Magazine 154, 1344-1359.

Wei, G.-Y., Planavsky, N.J., Tarhan, L.G., Chen, X., Wei, W., Li, D., Ling, H.-F., 2018. Marine redox fluctuation as a potential trigger for the Cambrian explosion. Geology 46, 587-590.

Wei, G.-Y., Wei, W., Wang, D., Li, T., Yang, X., Shields, G.A., Zhang, F., Li, G., Chen, T., Yang, T., Ling, H.-F., 2020. Enhanced chemical weathering triggered an expansion of euxinic seawater in the aftermath of the Sturtian glaciation. Earth and Planetary Science Letters 539, 116244.

Weyer, S., Anbar, A.D., Gerdes, A., Gordon, G.W., Algeo, T.J., Boyle, E.A., 2008. Natural fractionation of $^{238}U/^{235}U$. Geochimica et Cosmochimica Acta 72, 345-359.

Wood, R., Bowyer, F., Penny, A., Poulton, S.W., 2018. Did anoxia terminate

Ediacaran benthic communities? Evidence from early diagenesis. Precambrian Research 313, 134-147.

Wood, R., Erwin, D.H., 2018. Innovation not recovery: dynamic redox promotes metazoan radiations. Biol. Rev. Camb. Philos. Soc. 93, 863-873.

Wood, R., Liu, A.G., Bowyer, F., Wilby, P.R., Dunn, F.S., Kenchington, C.G., Cuthill, J.F.H., Mitchell, E.G., Penny, A., 2019. Integrated records of environmental change and evolution challenge the Cambrian Explosion. Nat. Ecol. Evol. 3, 528-538.

Xu, L., Lehmann, B., Mao, J.,Qu, W., Du, A., 2011. Re-Os Age of Polymetallic Ni-Mo-PGE-Au Mineralization in Early Cambrian Black Shales of South China--A Reassessment. Economic Geology 106, 511-522.

Zhang, F., Xiao, S., Kendall, B., Romaniello, S.J., Cui, H., Meyer, M., Gilleaudeau, G.J., Kaufman, A.J., Anbar, A.D., 2018. Extensive marine anoxia during the terminal Ediacaran Period. Science Advances 4, eaan8983.

Zhang, F., Xiao, S., Romaniello, S.J., Hardisty, D., Li, C., Melezhik, V., Pokrovsky, B., Cheng, M., Shi, W., Lenton, T.M., Anbar, A.D., 2019. Global marine redox changes drove the rise and fall of the Ediacara biota. Geobiology 17, 594-610.

Figure captions

Figure 1. Stratigraphic columns of the Daotuo drill core and Yanjia sections, and their correlations to inner shelf Xiaotan section and Gaojiaxi–Yanjiahe section in South China (cf. Wei et al., 2018). The shaded areas represent the correlative stratigraphic units of these sections for the Ediacaran (blue), Cambrian Fortunian and Stage 2 (green) and Stage 3

(yellow). The red line represents a Ni-Mo polymetallic layer with an age of 521± 5 Ma (Re-Os dating from Xu et al., 2011) or < 522.7 ± 4.9 Ma (U-Pb zircon dating from Wang et al., 2012).

Figure 2. Uranium isotope ($\delta^{238}U_{auth}$) values, iron speciation, U_{auth} concentrations and total organic carbon (TOC) contents of the upper Ediacaran to lower Cambrian Daotuo drill core and Yanjia section. Uranium isotope values are presented as $\delta^{238}U_{auth}$ for authigenic uranium in bulk samples. The $\delta^{238}U_{auth}$ calculation are shown in Supplementary materials. The error bar represents an overall uncertainty (2SD) of calculated $\delta^{238}U_{auth}$ for each sample, using a Monte Carlo approach. The shaded vertical bars are estimated average $\delta^{238}U$ ranges of suboxic and euxinic sediments (Andersen et al., 2017).

Figure 3. Cross-plots of (A) bulk U concentration vs. Al concentration, (B) bulk $\delta^{238}U$ vs. Al concentration, (C) bulk U concentration vs. Th concentration, (D) bulk $\delta^{238}U$ vs. Th concentration for samples from the Daotuo drill core and Yanjia section. R^2 represents the coefficient of determination of the covariation.

Figure 4. Cross-plots of (A) authigenic U concentration vs. Fe concentration, (B) authigenic $\delta^{238}U$ vs. Fe concentration, (C) authigenic U concentration vs. TOC concentration, (D) authigenic $\delta^{238}U$ vs. TOC concentration for samples from the Daotuo drill core and Yanjia section. R^2 represents the coefficient of determination of the covariation.

Figure 5. (A) Fe_{HR}/Fe_T vs. Fe_{Py}/Fe_{HR} for the samples from the Daotuo drill core and Yanjia section analyzed in this study. The divisions between oxic and anoxic conditions (Fe_{HR}/Fe_T = 0.22–0.38) and between ferruginous and euxinic conditions (Fe_{Py}/Fe_{HR} = 0.7–0.8) are derived from Poulton and Canfield (2011). (B) Cross-plots of Mo_{EF} vs. U_{EF} for the samples from the

Daotuo drill core and Yanjia section in this study as a proxy for local marine sedimentary environment. The shaded zones for different sedimentary environment of the modern ocean are modified after Algeo and Tribovillard (2009) and Tribovillard et al. (2012). Particulate shuttle zone: the transport of Mo within the water column by Fe-Mn-oxyhydroxide particulates (e.g., as in the Cariaco Basin); Open marine zone: benthic redox variations in modern open-ocean systems; Strongly restricted basin: sedimentary basin weakly connected to the open-ocean (e.g, as in the Black Sea).

Figure 6. Cross-plots of (A) authigenic $\delta^{238}U$ vs. Fe_{HR}/Fe_T, (B) authigenic $\delta^{238}U$ vs. Fe_{Py}/Fe_{HR} for the samples in the Daotuo drill core and Yanjia section.

Figure 7. (A)–(B) Secular changes in U isotopic compositions of carbonates (data from Wei et al., 2018; Zhang et al., 2018; Tostevin et al., 2019; Dahl et al., 2019) and siliciclastic rocks from the late Ediacaran to early Cambrian. (C) Calculated $\delta^{238}U_{SW}$ values derived from $\delta^{238}U_{auth}$ records in this study. The solid curves are LOWESS smoothing fits for U isotope data. Based on TOC, Mo_{EF}–U_{EF} and Fe speciation analyses, U isotopic differences between reducing sediment and seawater are estimated to be +0.8‰ for organic-rich anoxic or sulfidic samples with TOC > 5 wt% and Mo_{EF} and U_{EF} > 20 (purple circles); +0.6‰ for anoxic samples with TOC < 5wt%, Mo_{EF} and U_{EF} >10 (orange circles); and +0.15‰ for potentially suboxic samples with Mo_{EF} and U_{EF} < 10 (gray circles). The shaded vertical bars are estimated average $\delta^{238}U$ ranges of modern non-skeletal carbonates, suboxic sediments and euxinic sediments (Andersen et al., 2017). N1–N3 and P1–P3 represent negative and positive U isotopic excursions from the late Ediacaran though the early Cambrian.

Figure 1

Click here to download Figure: Figure 1_R1.pdf

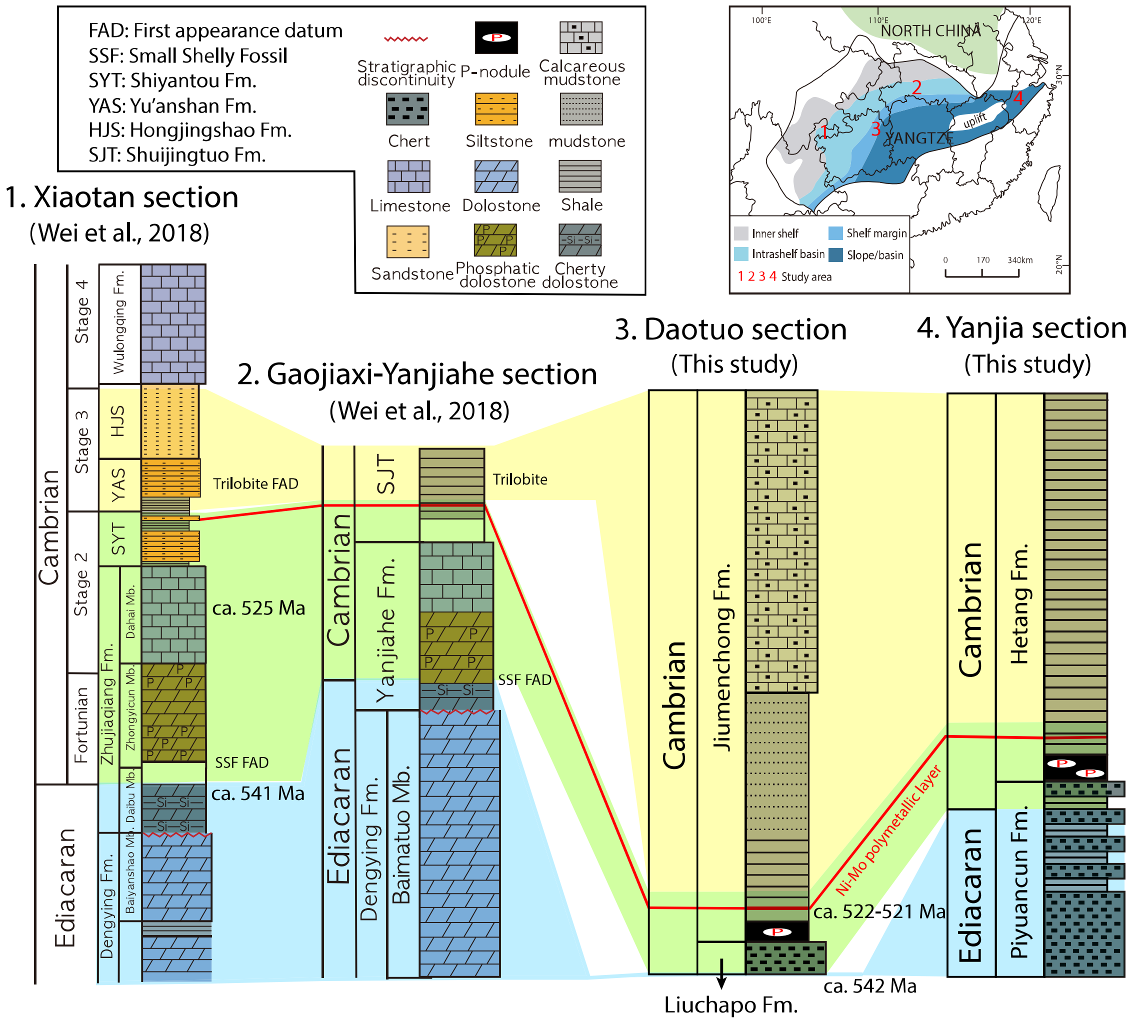

Figure 2

Click here to download Figure: Figure 2_R1.pdf

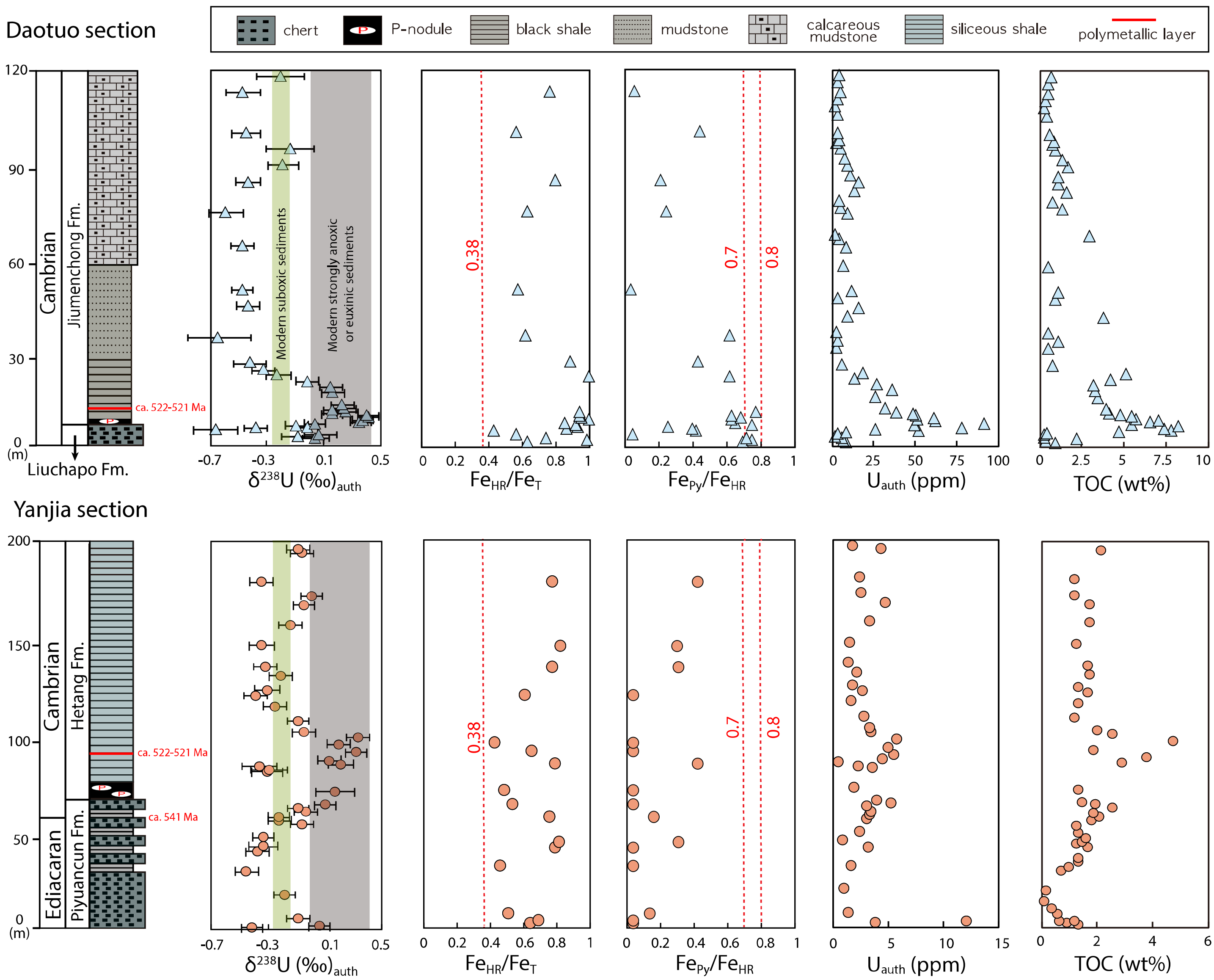

Figure 3

Click here to download Figure: Figure 3_R1.pdf

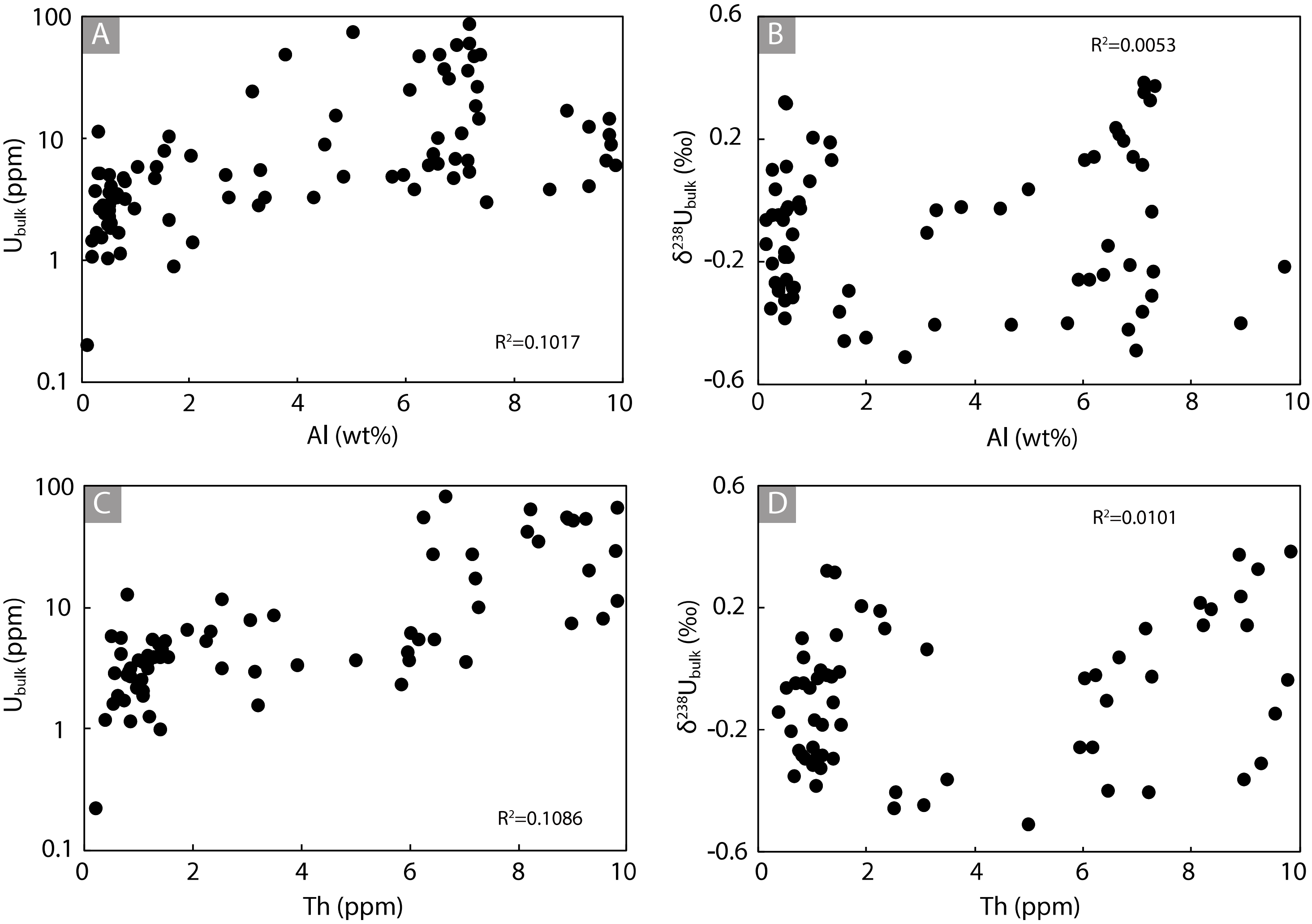

Figure 4
Click here to download Figure: Figure 4_R1.pdf

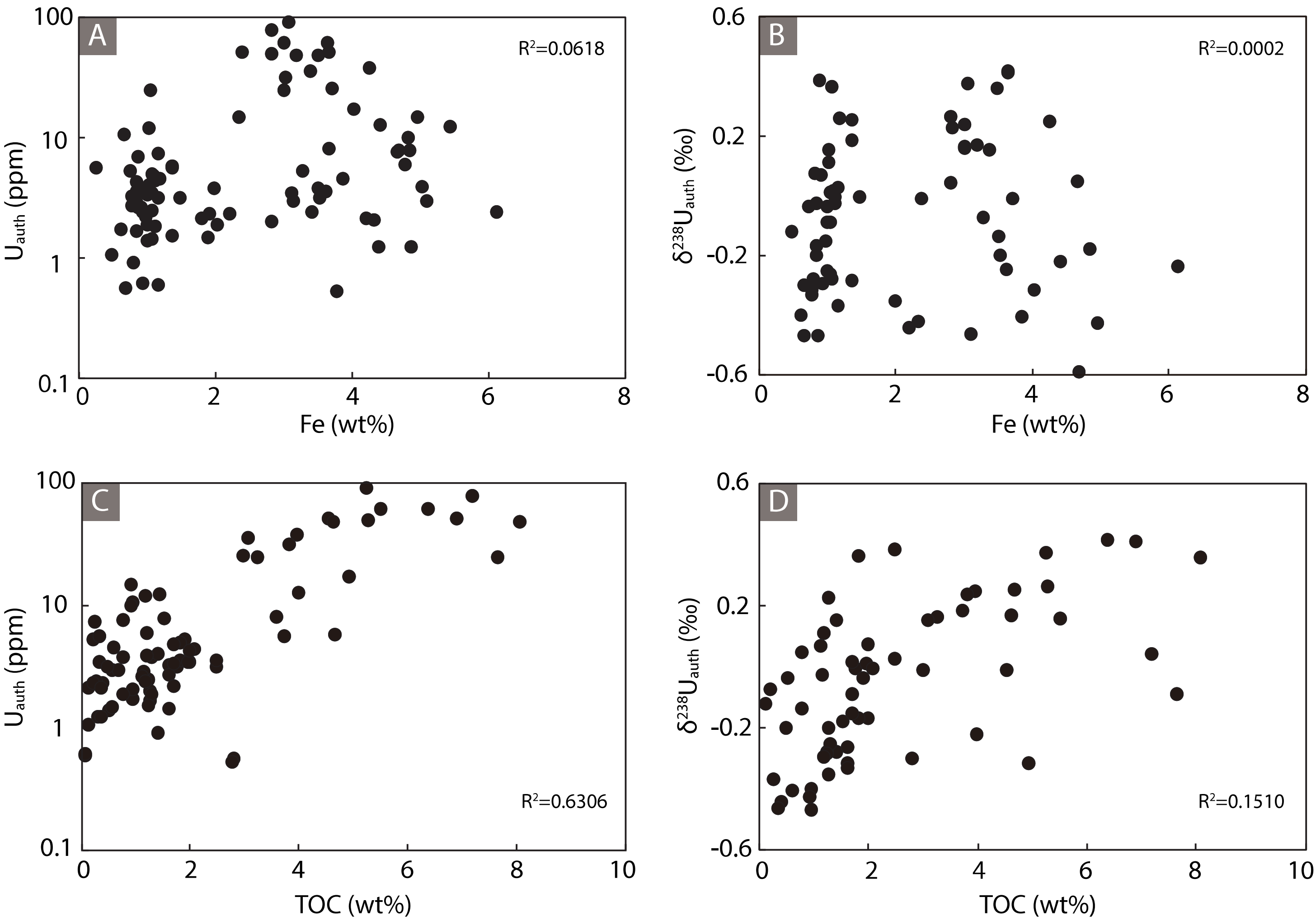

Figure 5

Click here to download Figure: Figure 5_R1.pdf

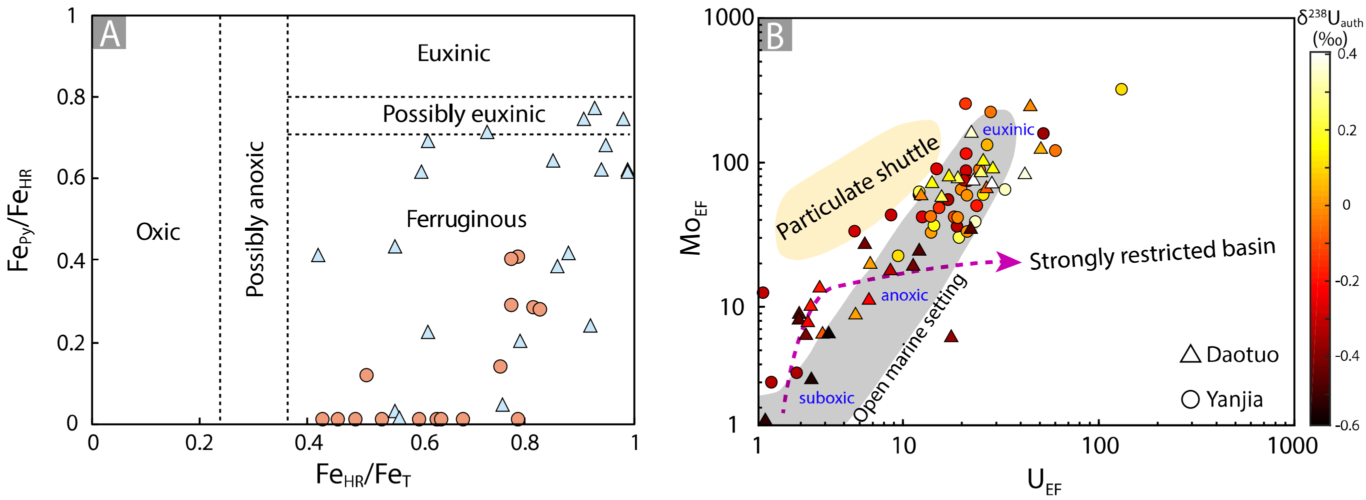

Figure 6

Click here to download Figure: Figure 6_R1.pdf

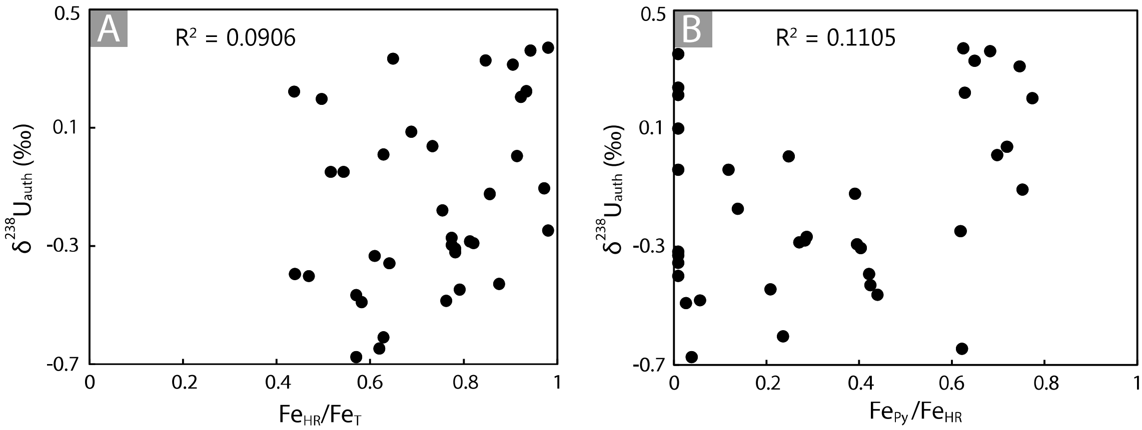

Figure 7

Click here to download Figure: Figure 7_R1.pdf

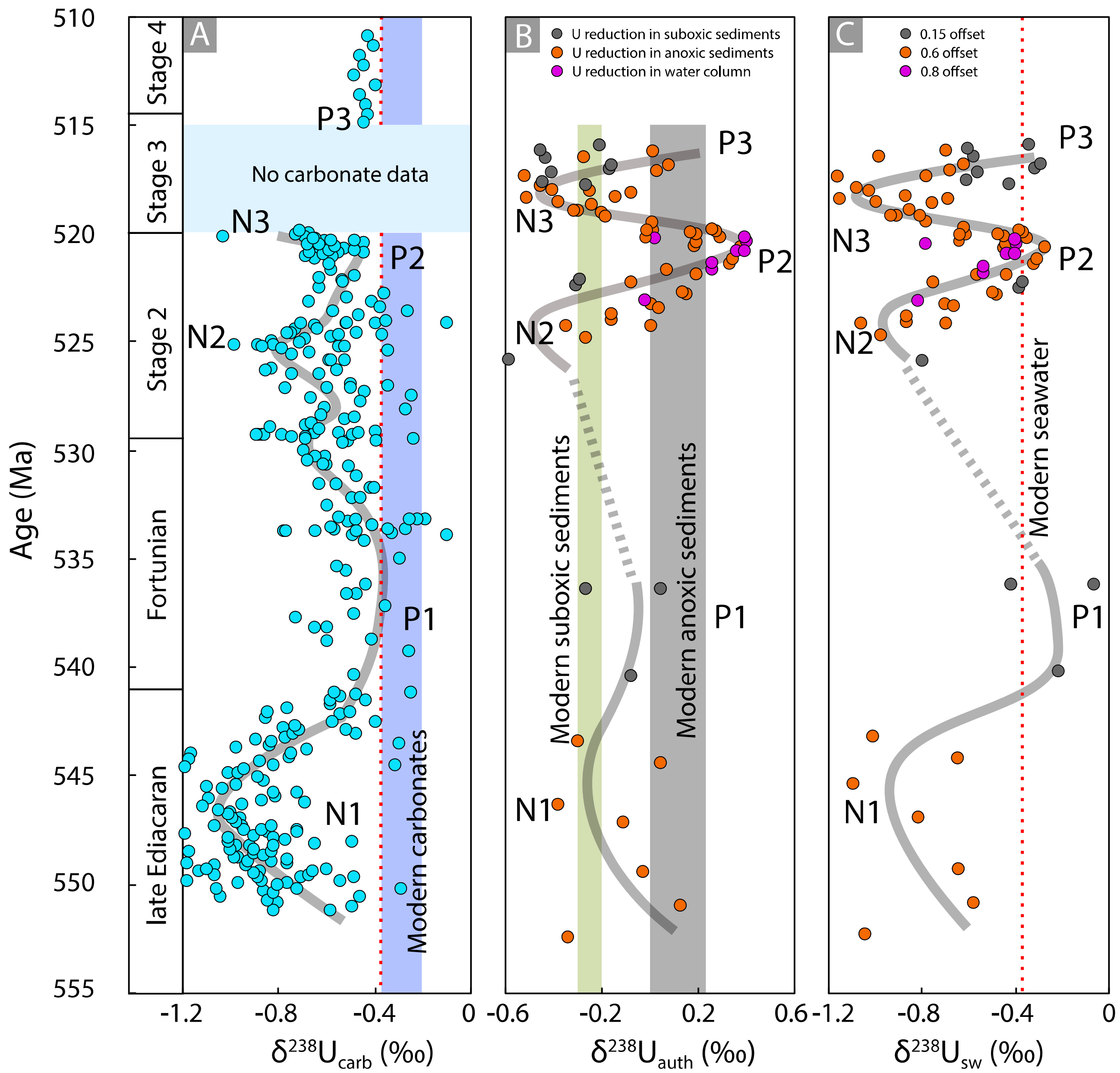

***Credit Author Statement**

CRediT author statement

Guang-Yi Wei: Conceptualization, Resources, Methodology, Investigation, Writing-Original draft, Writing-Reviewing and Editing.
Noah Planavsky: Conceptualization, Investigation, Writing-Reviewing and Editing
Lidya Tarhan: Investigation, Writing-Reviewing and Editing
Tianchen He: Resources, Investigation
Graham A. Shields: Writing-Reviewing and Editing
Wei Wei: Resources
Dan Wang: Resources
Hong-Fei Ling: Conceptualization, Writing-Original draft, Writing-Reviewing and Editing

*Declaration of Interest Statement

The authors declare that they have no known competing financial interests or personal relationships that could have appeared to influence the work reported in this paper.